NASA CONTRACTOR REPORT

NASA CR-1881

TRAFFICABILITY AND VISIBILITY ANALYSIS OF THE LUNAR SURFACE

by H. T. McAdams, P. A. Reese, and G. M. Lewandowski

Prepared by
CORNELL AERONAUTICAL LABORATORY, INC.
Buffalo, N.Y. 14221
for George C. Marshall Space Flight Center

NATIONAL AERONAUTICS AND SPACE ADMINISTRATION • WASHINGTON, D. C. • JULY 1971

1. REPORT NO.	2. GOVERNMENT ACCESSION NO.	3. RECIPIE
NASA CR-1881		

4. TITLE AND SUBTITLE	5. REPORT DATE
TRAFFICABILITY AND VISIBILITY ANALYSIS OF THE LUNAR SURFACE	July 1971
	6. PERFORMING ORGANIZATION CODE

7. AUTHOR(S)	8. PERFORMING ORGANIZATION REPORT #
H. T. McAdams, P. A. Reese, and G. M. Lewandowski	

9. PERFORMING ORGANIZATION NAME AND ADDRESS	10. WORK UNIT NO.
Cornell Aeronautical Laboratory, Inc. Buffalo, New York 14221	914-40-42-0062
	11. CONTRACT OR GRANT NO.
	NAS8-26251
	13. TYPE OF REPORT & PERIOD COVERED
12. SPONSORING AGENCY NAME AND ADDRESS	CONTRACTOR REPORT
NASA Washington, D. C. 20546	14. SPONSORING AGENCY CODE

15. SUPPLEMENTARY NOTES

Technical Coordinator: O. H. Vaughan, Jr.

16. ABSTRACT

Cornell Aeronautical Laboratory, Inc. (CAL) under contract to the Aerospace Environment Division, Aero-Astrodynamics Laboratory, Marshall Space Flight Center, has developed computerized methods for trafficability and visibility analysis for use in lunar surface mission planning, using either manned or unmanned roving vehicles. The Fra Mauro area was selected as the site to be analyzed using these techniques, since the Apollo 14 mission scheduled to land in this area could help to verify many assumptions developed during this study regarding the lunar surface roughness characteristics as seen during surface operations. Trafficability and visibility maps were successfully produced based on the available data for the site.

17. KEY WORDS	18. DISTRIBUTION STATEMENT
Trafficability and Visibility Modeling	

19. SECURITY CLASSIF. (of this report)	20. SECURITY CLASSIF. (of this page)	21. NO. OF PAGES	22. PRICE
Unclassified	Unclassified	78	$3.00

Acknowledgments

The authors acknowledge the leadership and guidance of the sponsor, Mr. O. H. Vaughan, Jr., Aerospace Environment Division, Aero-Astrodynamics Laboratory, Marshall Space Flight Center, who conceived the study problem and provided the necessary lunar surface reference materials and Lunar Roving Vehicle characteristics to be used in this study.

A number of individuals, in addition to those named as authors of this report, have contributed significantly to the accomplishments of the study. Dr. W. F. Wood provided much-needed guidance in the analysis and interpretation of source data and was responsible for effort aimed at the possible use of a horizon graphic as a navigation aid. W. C. Grenke and C. J. Nuttall, Jr., of WNRE, Inc., developed the basic trafficability model on which the trafficability maps are based; their contributions constitute a major part of Appendix I. C. Groenewoud developed the basic visibility model called ASTERISK; Appendix II is based largely on his contributions. D.J. Schuring developed basic information and vehicle-terrain interaction concepts for energy-consumption analysis and authored Appendix III of this report. A.Guendel and J. Blickenstaff assisted in map digitization and data key punching, and J. Yannitell typed the report manuscript.

TABLE OF CONTENTS

		Page
1.	INTRODUCTION	1
	1.1 Trafficability Maps	1
	1.2 Visibility Maps	4
	1.3 Graphic Representation of the Horizon	8
2.	INPUT CONSIDERATIONS	9
	2.1 Lunar Terrain Inputs	9
	2.1.1 Total Surface Characteristics	12
	2.1.2 Detailed Surface Characteristics	13
	2.2 Vehicle Inputs	17
3.	EVALUATION MODEL CONSIDERATIONS	19
	3.1 Trafficability Model	19
	3.2 Visibility Model	22
4.	OUTPUT CONSIDERATIONS	23
5.	RESULTS	24
	5.1 Trafficability Maps	24
	5.2 Visibility Maps	28
	5.3 Horizon Graphics	33
6.	CONCLUSIONS, RECOMMENDATIONS AND PROSPECTUS	36
APPENDIX I	Trafficability Computer Program Documentation	38
APPENDIX II	Landmark Visibility Computer Program Documentation	50
APPENDIX III	Vehicle Soft-Soil Performance Modeling	63

LIST OF FIGURES

Figure		Page
1	Trafficability Analysis	3
2	Schematic for the Computer Generation of Visibility Maps	5
3	Composite Visibility Map	7
4	Processing of Unit Terrains	20
5	Line-of-Sight "Search" Procedure	22
6	Area Mapped for Trafficability	25
7	Computer Print-out of Trafficability Map	26
8	Go/No-Go Map with Overlays	27
9	Computer Print-out of Visibility Map	29
10	Computer Print-out of Visibility Map	30
11	Computer Print-out of Visibility Map	31
12	Visibility Map with Overlays	32
13	Computer Print-out of Visibility Map	34
14	Visibility Map with Overlay	35

LIST OF TABLES

Table		Page
I	Source Material	10
II	Codes Used for Slopes of Craters Greater Than 50 Meters Diameter, Soil Firmness, and Age of Craters Less Than 50 Meters in Diameter	15
III	Lunar Vehicle Data for Locomotion Analysis	17
IV	Performance Tests of Vehicle-Terrain Compatibility	20

I. INTRODUCTION

This research program was undertaken to provide the Aerospace Environment Division, Aero-Astrodynamics Laboratory, Marshall Space Flight Center, with techniques which could help to better define the trafficability and visibility problems which might be encountered by a manned or unmanned Lunar Roving Vehicle carrying out a scientific mission on the lunar surface. The landing site for the Apollo 13 mission was selected and Orbiter data was used as the baseline in this study since the Apollo 14 site was in the same area and the topographic data needed for the study and for generation of a new map was in a state of re-evaluation based on better photography from the Apollo 12 mission.

1.1 Trafficability Maps

The concept of a trafficability or "going" map as an assist to the operational use of vehicles is well established on the earth. For example, extensive series of Cross-Country Movement (CCM) maps have been produced for both tactical and strategic planning for many areas of the earth's surface. These maps are based on the capabilities of a typical tracked or wheeled vehicle and the challenge presented by the integrated effects of surface geometry and composition, vegetation, hydrological features, and cultural modifications of the terrain. For a typical vehicle, the maps classify and display areas according to the ease with which they can be negotiated. These classes are generally qualitative rather than quantitative, in the sense that they classify areas nominally as "good", "fair", "poor", etc. from the standpoint of traversability. By means of methods developed at Cornell Aeronautical Laboratory, such maps can be produced by computer-aided techniques.[1] In this way, a variety of maps can be generated, each displaying relevant information in a form particularly suited to the problem at hand.

Under previous Contract No. NAS8-25110, Cornell Aeronautical Laboratory, Inc. (CAL) considered hazards to movement for a proposed Dual

(1) H.T.McAdams, Computer Mapping and Data Presentation, Technical Memorandum No. VJ-2330-G-55, Cornell Aeronautical Laboratory, Inc., Buffalo, N.Y. (1969).

Mode Lunar Roving Vehicle.[2] This project was denoted as Moon River I and will often be subsequently referred to in this report by that name. A companion program was conducted by WNRE, Inc. under Contract No. NAS8-25137.[3] The objective of these programs was to prepare, for specific area of the lunar surface, located in Sinus Medii, a set of maps identifying sites where a vehicle might be stopped or its progress seriously hampered. It was expected that such an analysis, in addition to serving as an aid to maneuvering the vehicle the vehicle, would also assist in designing a vehicle having the desired capability to negotiate the lunar terrain.

Vehicle-terrain interaction models and computerized mapping techniques developed under Contracts NAS8-25110 and NAS8-25137 and applied to the Dual Mode vehicle were seen to be applicable to the Manned Lunar Rover. The trafficability aspect of the work reported herein relies heavily on the methods and procedures of the previous contracts.

The basic scheme for trafficability analysis is shown in Figure 1. Factors affecting the performance of the Manned Lunar Rover include slope of the terrain, crater characteristics, soil strength, and the presence or absence of such obstacles as blocks and lineal features. These terrain features are abstracted from maps and photographs of the lunar surface, expressed in digital form and converged into "unit terrains" representing specific types of challenges to the vehicle. By means of a vehicle-terrain interaction model developed by WNRE, Inc. and modified by CAL, the terrain demands are compared with vehicle capability. The results, expressed as a code denoting whether a specific location represents a Go, No-Go, or conditional Go situation, are then printed out as a trafficability map.

---

(2) W.F. Wood and G.M. Lewandowski, Maneuvering the Dual Mode Manned/Automated Lunar Roving Vehicle, Report No. VS-2860-D, Cornell Aeronautical Laboratory, Inc., Buffalo, N.Y. (1970) (MOON RIVER I Final Report)

(3) W.C. Grenke and C.J. Nuttall, Jr., Accessibility of Specific Areas on the Lunar Surface as a Function of LRV Mobility Design Parameters, Report No. 201, WNRE, Inc., Chestertown, Maryland (1970).

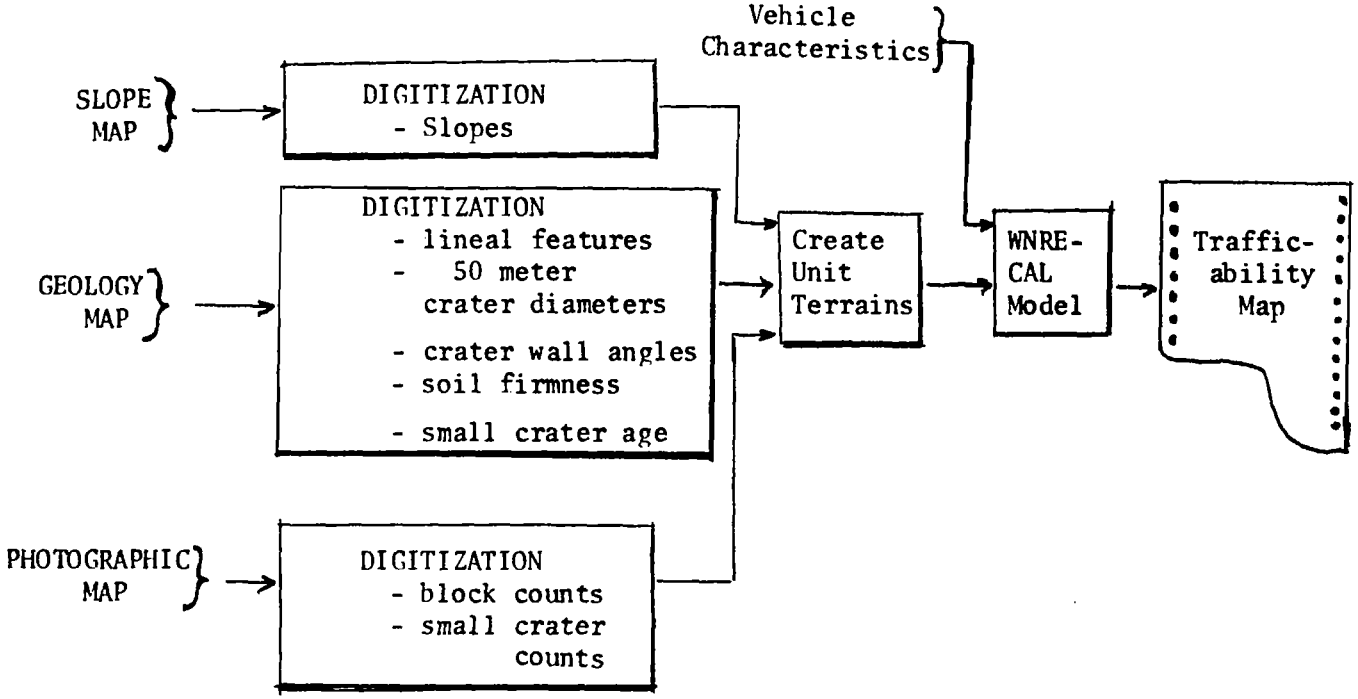

FIGURE 1

TRAFFICABILITY ANALYSIS

1.2 Visibility Maps

It is recognized that the ability of a vehicle to negotiate the lunar terrain does not entirely determine the nature of the missions which might be performed. Line-of-sight visibility might well play an important role, because of the risks involved in maneuvering in a terrain where visibility is limited. In particular, ability to navigate might be degraded significantly if line-of-sight visibility is restricted. It was accordingly desired to develop maps which delineate regions wherein specified landmarks are visible. In addition, it was proposed to develop, by computer display, representations of the horizon as seen from specified locations.

Line-of-sight analyses have been performed extensively at Cornell Aeronautical Laboratory, Inc. in connection with problems in air defense. For example, if an air defense site is located at a certain point on a map, the points visible or not visible from that site can be mapped in much the same way as the areas of Go or No-Go are mapped for a vehicle. It is important to note the important distinction, however, that the masked and non-masked areas relate only to a fixed point of observation. If the observation point is moved to a new location, a completely different map evolves.

The problem of landmark visibility, as presented in map form, is more or less the inverse of the type of line-of-sight analysis required in problems of air defense. In that application, the viewing point P is fixed, and the point observed, call it Q, is variable. In the case of landmark visibility, the point to be observed is fixed, and the viewing point is variable. Since line-of-sight from P to Q implies line-of-sight from Q to P, however, it is a straightforward matter to develop a map which separates all possible viewing points into two categories, SEE and NO-SEE (or, "unmasked" and "masked"). For a given landmark, therefore, the resulting map takes a form completely analogous to a Go/No-Go trafficability map.

Figure 2 is a schematic of the procedure used to generate visibility maps. Here terrain elevations are the only lunar features to be considered.

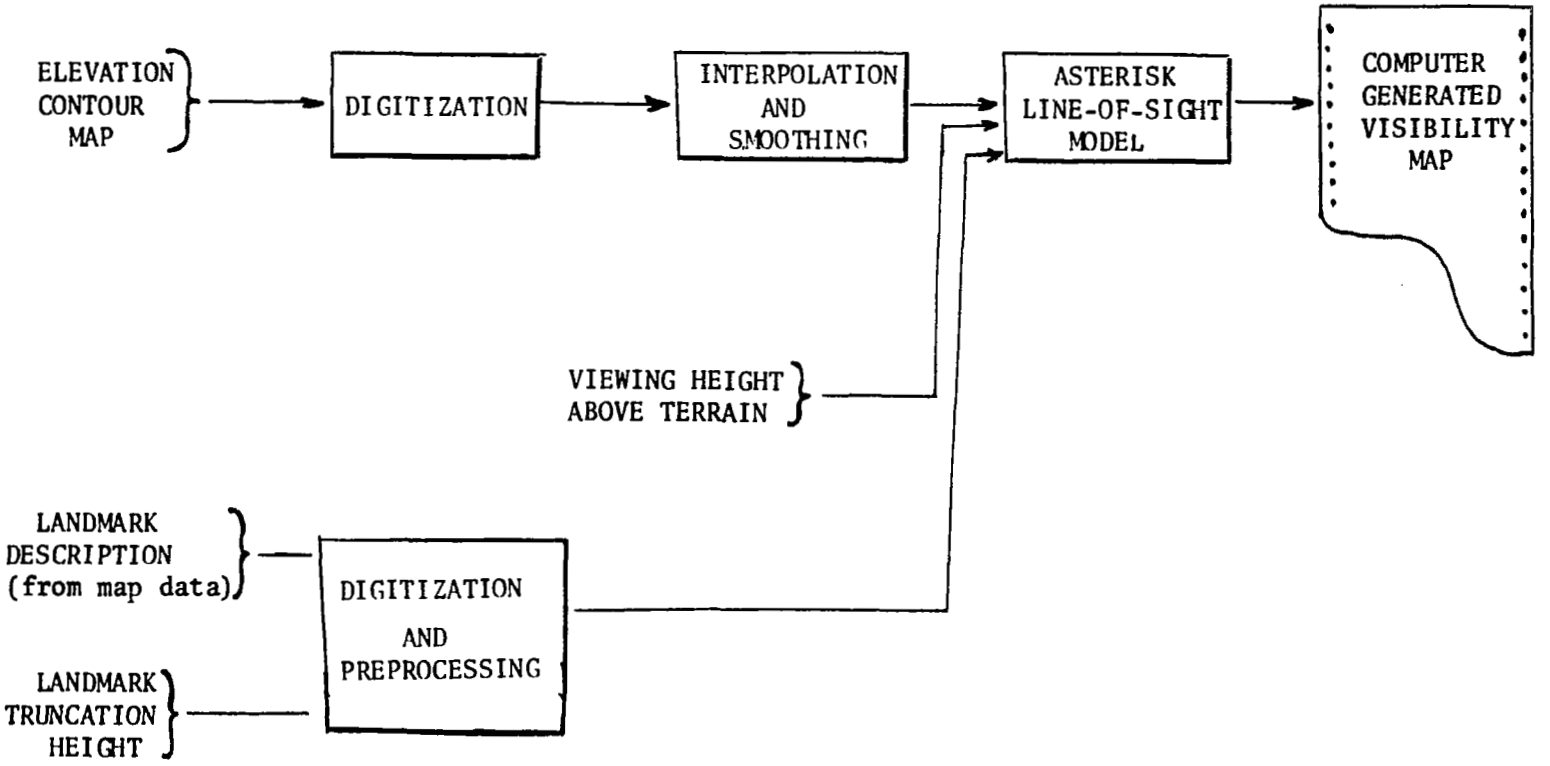

FIGURE 2

SCHEMATIC FOR THE COMPUTER GENERATION OF VISIBILITY MAPS

The elevations are taken from a contour map of the lunar surface and, after being digitized, are smoothed to eliminate discontinuities resulting from the discreteness of the digitization. A selected landmark is also digitized and, by appropriate data preprocessing, described in terms suitable for data processing by the computer model. Part of this preprocessing involves a "truncation" of the landmark feature at some level below its uppermost elevation. Such truncation assures that the landmark will not only be seen but that a sufficient extent of it will be visible to make its identification possible.

If landmarks are to be used to assist in locating position on the moon's surface, it is desirable to be able to identify more than one landmark. If three or more landmarks are visible, they constitute in essence a coordinate system to which the viewing point can be referred. Therefore it was considered possible to develop, for the sites of interest, maps which designate the areas wherein all three (or more) landmarks are visible.

Consider three landmarks A, B, and C. For landmark A, one can develop a SEE/NO-SEE map as shown schematically in Figure 3-A. To produce such a map, it is necessary only to lay out a grid and to examine each grid point to determine if line-of-sight exists from the grid point to the landmark. If line-of-sight exists, the corresponding grid square is left blank. If line-of-sight does not exist, the corresponding grid square is filled by the symbol A. Similarly, one can develop, independently, a SEE/NO-SEE map for landmarks B and C, as shown in Figure 3-B and 3-C. To obtain a map showing those areas in which all three landmarks are simultaneously visible, it is necessary only to intersect or overlay the three maps, as shown in the composite map, Figure 3-D. The resulting clear areas are those areas within which all three landmarks are visible. Areas occupied by A, B or C or any combination thereof do not satisfy the criterion of simultaneous visibility of all three landmarks (although they might allow visibility of one or two of the landmarks). The overlaying process can be executed by means of transparencies or in the computer by the process of logical intersection. As is evident, the choice of symbology is not limited to letters such as A, B, C; various types of shading or cross-hatching, as well as different colors, can be employed. Also, it is evident that the number of maps intersected is not limited. Conceptually, any number of landmarks could be examined and a composite map developed.

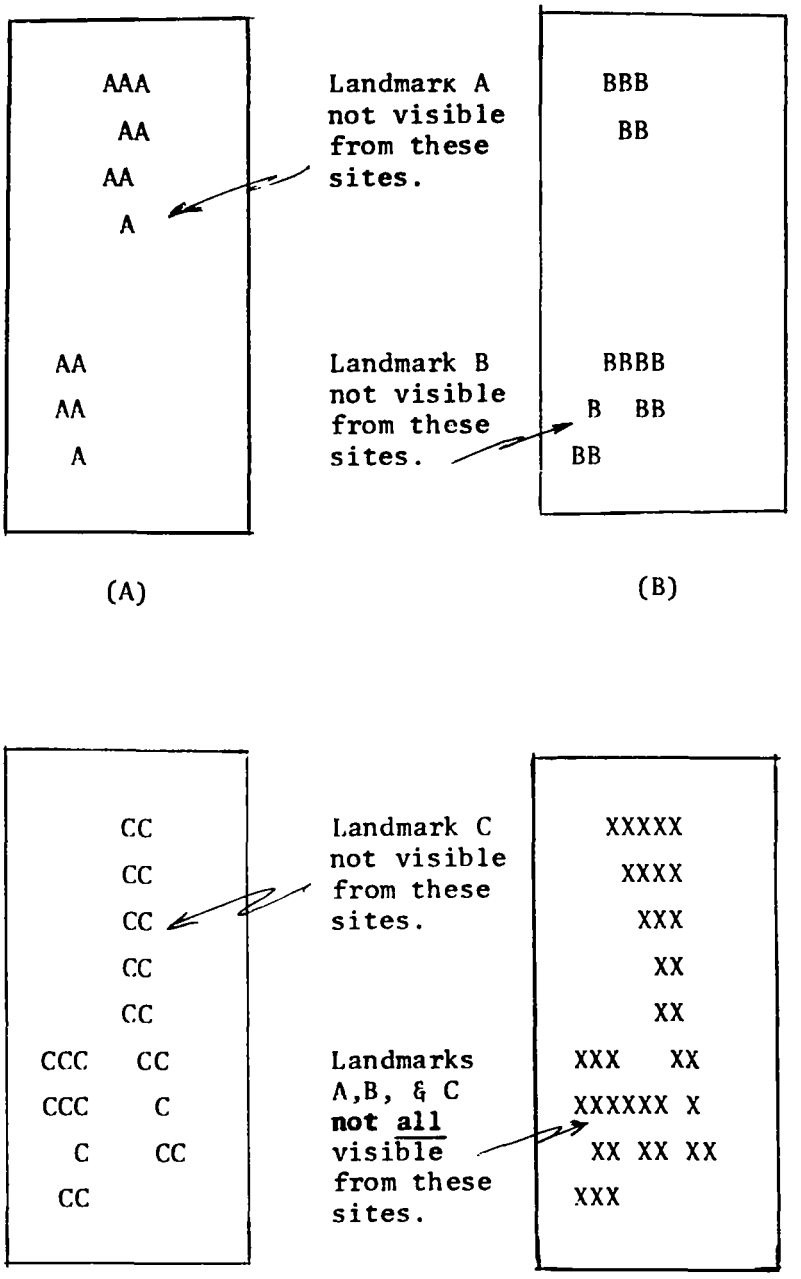

FIGURE 3

COMPOSITE VISIBILITY MAP

It is self-evident that landmarks should be chosen in such a way that they are visible over a large percentage of the area. Ideally, it would be desirable to have all of the landmarks visible from everywhere in the area of operation. If such were the case, the landmark visibility map would degenerate to the trivial case in which all of the area is free of nonvisibility symbols. It should also be borne in mind that one of the best choices of a landmark is the lunar module and that if this landmark were everywhere visible, there would be little need for other landmarks except as supplementary points of reference for added protection.

1.3 Graphic Representation of the Horizon

If line-of-sight were the most important consideration in a lunar mission, the lunar module could possibly be landed in a location where it could be seen from nearly anywhere in the study area. However, for a number of reasons such a choice of landing site would seldom, if ever, be possible. Therefore, landmarks on the horizon as well as those within the study area were considered potentially useful to the astronauts in orienting themselves. The horizon as seen from the center of Copernicus could be as far as 50 km. away, yet provide distinct landmarks. Accordingly, part of the effort under this program was aimed at exploring the extent to which the horizon might be useful as a position reference on the lunar surface.

2. INPUT CONSIDERATIONS

To evaluate the degree of match or mismatch between the Manned Lunar Rover and the lunar terrain requires that both be described in terms of parameters which are capable of being compared in a meaningful way. A series of comparisons, or "tests" can then be made to judge whether the vehicle is or is not compatible with the terrain at a given location.

A terrain classification for lunar features was previously developed under Contract NAS8-25110.[4] For purposes of the present study, it was necessary to modify the terrain classification to some extent and to incorporate some terrain features which were not required in the earlier work. First, Fra Mauro is a more diversified terrain than Sinus Medii. Second, in order to conduct a line-of-sight analysis, considerable emphasis on surface elevations and their quantitative representation was required.

2.1 Lunar Terrain Inputs

Digitization of lunar surface characteristics was carried out for two specific purposes: (1) to produce computer drawn maps which would aid in assessing trafficability, and (2) to produce maps showing the visibility of specific landmarks from the lunar landing site and from other points on the EVA routes.

Source material made available by the sponsor for use in the study is listed in Table I. The area of the moon, to be examined in producing trafficability and visibility maps is contained in the Fra Mauro Contour Manuscript (5-meter contour interval). The coordinates of the approximate center of the study area are:

3° 24' South
17° 20' West

---

(4) W.F. Wood and G.M. Lewandowski, op. cit.

TABLE I

SOURCE MATERIAL

1. Photo Base for Fra Mauro contour manuscript (5 meter), Approx.scale 1:13,720
   1(a) through 1(e) are transparent overlays based on the above.

   1(a). Plate I Topographic map, 5 meter intervals
   1(b) Plate II Slope map 5° intervals
   1(c) Plate III Preliminary geologic map
   1(d) Plate IV Terrain classification map (Theoretical LRV traverse route)
   1(e) Plate V Topographic profiles and comparison of photoclinometric and photogrametric reduction.

2. Geologic map of the Fra Mauro landing site-Apollo 13, scale 1:5000 by T.W.Offield, 1970; Base map prepared by USATPC for NASA.

3. Preliminary section to accompany geologic map of the Fra Mauro landing site-Apollo 13, 1:5000.

4. Geologic map of part of the Fra Mauro region of the moon-Apollo 13, by T.W. Offield, 1970, scale 1:25,000. Base map prepared by ACIC for NASA.

5. Geologic map of the Fra Mauro region of the moon-Apollo 13, by R.E.Eagleton. Scale 1:250,000, 1970. Base map prepared by ACIC for NASA.

6. Fra Mauro Pre-mission scheduled EVA's, approx. scale 1:10,000. Prepared by Mapping Sciences Laboratory, Science and Applications Directorate Manned Spacecraft Center, March 24, 1970.

7. Traverse Map-Apollo 13, Fra Mauro site; scale 1:2,500 (an enlarged orbiter photograph annotated with EVA route and science sites).

8. Lunar topographic map. Fra Mauro. (2nd Ed.) December 1969. Scale 1:250,000. Contour interval 200 m with supplementary contours at 100 m intervals. ACIC, USAF for NASA

9. Topographic Map (vicinity of Fra Mauro). Scale 1:25,000, contour interval 25 meters, February 1970. Dept. of Interior, USGS, Center of Astrogeology, Flagstaff, Arizona.

10. Fra Mauro Lunar topographic photomap. Scale 1:25,000, contour interval 10 meters. February 13, 1970. Mapping Science Laboratory, Science and Application Directorate NASA MSC.

11. Lunar Orbiter IV Photograph IV. 120 H_3. NASA LRC version. Approx. scale 1:10,000.

12. Lunar Orbiter, Photograph III, 133 H_2, III 133 H_3, NASA LRC version. Approx. scale 1:10,000.

13. Lunar Orbiter III, USGS Rectified photo mosaic from LO III H-133, scale 1:5000.

14. Lunar Photomap Fra Mauro, scale 1:250,000.(1st Ed.1969) Prepared by ACIC for NASA.

15. Apollo Photographs. Ground views showing astronauts, LEM, Surveyor, and Panoramic views. 15 8"x10" glossy prints.

Two general categories of lunar surface characteristic data were considered:

1. Total Surface Characteristics
   a. Lunar surface elevations
      (Fra Mauro contour manuscript-- topographic map-- 5 meter contour interval)
   b. Maximum gross slope
      (Fra Mauro contour manuscript -- Slope map-- 5 degree slope intervals)
   c. Soil firmness
      (Geologic Map of the Fra Mauro Landing Site-- Apollo 13-- Scale 1:5,000 by T.W.Offield 1970, and Moon River I-Final Report, Table 7)

2. Detailed Surface Characteristics
   a. Crater information
      i) Diameters of craters having diameters greater than 50 meters (Geologic map of the Fra Mauro landing site - Apollo 13- Scale 1:5,000 by T.W. Offield 1970)
      ii) Crater wall angle for craters having diameters greater than 50 meters. (Geologic Map of the Fra Mauro Landing Site-- Apollo 13 - Scale 1:5,000, by T.W. Offield 1970, and Moon River I - Final Report, Table 7)
      iii) Crater counts, 5-20 meters in diameter and 20-50 meters in diameter. (NASA-LRC Lunar Orbiter-Mission III, high resolution photographs)
      iv) Age of small craters (less than 50 meters in diameter)
   b. Density of Lineal Features
      (Geologic Map of the Fra Mauro Landing Site - Apollo 13- Scale 1:5,000, by T.W. Offield, 1970)
   c. Block Count (down to resolution size)
      (NASA-LRC Lunar Orbiter - Mission III, high resolution photographs).

A grid system having a fifty-meter spacing and employing boundaries parallel to the latitude and longitude coordinate lines of the approximate center of the study area was devised to aid in the data collection. This coordinate system covers most of the mapped area and is 160 points by 260 points in grid-square

dimensions. Each type of data, whether point-collected data or area-collected data, were gathered in an orderly fashion from the locations on this grid system.

2.1.1 Total Surface Characteristics

a. Lunar Surface Elevation

Lunar surface elevations were read at all points on the coordinate system. The map used had a contour interval of 5 meters over most of the area, with the exception of some steep, inner crater walls which were contoured at 25 meters. Even though a few exceptions existed, it was decided to read elevations to within 5 meters. This procedure necessitated making an estimate of the elevation between contours in areas where the contour interval was greater than 5 meters. It also created the problem of having the same elevation value for groups of points in areas where contours were spaced relatively far apart.

b. Maximum Gross Slope

Maximum gross slope values were read from the slope map furnished by the sponsor. This map indicated a range of slope, in 5° intervals, for specific areas within the study region. The maximum value within the range of slope was collected at each grid coordinate.

The intervals and codes used were:

Code	Slope	Sloped Used
1	0° - 5°	5°
2	5° - 10°	10°
3	10° - 15°	15°
4	>20°	25°

c. Soil Firmness

The soil firmness index contains information which attempts to describe lunar surface material in terms of a soil strength gradation (1 through 6, with 1 being the firmest). A survey carried out on Moon River I under Contract NAS8-25110 provided a relative classification of soil firmness for the Copernican System, Eratosthenian System, and background mare surface features. This same soil firmness index (Wood and Lewandowski, op.cit., pp.34-36) is used here. However,the Fra Mauro area contains some surface features of the Imbrian System. A literature search in terms of soil strength dealing with this system has not been made under the present study; hence, a relative value of soil firmness, as used on Moon River I, was not to be had for areas classified in the Imbrian System. The lack of a relative value of soil firmness is evidenced by the entrance of "0's" in the extended form of the soil firmness index mentioned above. When information about soil firmness of the Imbrian system classification types becomes available, a value in the scale from 1 to 6 can then be assigned. Whenever it became necessary to consider the Imbrian areas in the present study, however, as in the lunar mobility model, the value of 2 was assigned as a reasonably conservative estimate of soil strength. Although the Imbrian System areas of Fra Mauro resemble the background mare material of Sinus Medii, which was assigned the firmest soil classification, a more conservative value was considered appropriate for this mobility study.

2.1.2 Detailed Surface Characteristics

a. Crater Information

i) Diameter of craters having diameters greater than 50 meters.

A diameter code, explained below, was assigned to those grid squares falling within a crater having a diameter greater than 50 meters.

Code	Crater Diameter (Meters)
0	0 - 50
1	51 - 100
2	101 - 150
3	151 - 200
4	201 - 250
5	251 - 300
6	301 - 350
7	351 - 400
8	>401

ii) Crater wall angle for craters having diameters greater than 50 meters

The codes used for crater wall angle are shown below and are the same as used on Moon River I under Contract NAS8-25110 (Wood and Lewandowski, op.cit., p. 17)

Code	Slope
0	no craters or craters less than 50 meters
1	less than 2°
2	2° - 4° inclusive
3	5° - 6° inclusive
4	7° - 8° inclusive
5	9° -10° inclusive
6	11° -12° inclusive
7	13° -14° inclusive
8	over 14°

Additional information is found in Table II.

iii) Crater counts - 5 to 20 meters in diameter, and 20 to 50 meters in diameter

The crater counting procedures used to satisfy the WNRE trafficability model are somewhat different than those used on Moon River I. In that study, all craters within a size class were counted. However, computer-tabulated, crater-avoidance No-Go conditions indicated that only a few combinations of numbers of small and large craters would seriously affect mobility.

The following code, based on the No-Go conditions of crater avoidance, was developed and used.

No. of Craters of the Size 5-20 meters	No. of Craters of the Size 20-50 meters	Code
0	0	0
>1	0	1
0	1	2
>1	1	3
0	2	4
>1	2	5
≥10	2	6
0	3	7
>1	3	8

TABLE I1

CODES USED FOR SLOPES OF CRATERS GREATER THAN 50 METERS DIAMETER, SOIL FIRMNESS, AND AGE OF CRATERS LESS THAN 50 METERS IN DIAMETER.

Map Designation	Slope	Soil	Age
Cc6	7	5	1
6	7	5	1
Cc5	7	5	1
5	6	5	1
Cc4	5	4	2
4	3	2	2
Cc3	3	2	2
3	3	2	2
Cc2	3	2	3
2	2	2	3
Cc1	2	2	4
1	2	2	4
Ccd	3	6	4
Ech	2	2	4
Eci	2	2	4
Ecci	2	2	4
Ecc	2	1	4
Ec	2	1	4
Is	0*	0	4
Ifr	0*	0	4
Ifh	0*	0	4
Ic	0*	0	4
Slump	0*	5	-

* Use maximum gross slope classes

iv) Age of Small Craters

The age of small craters was assigned in the following manner.

Code	Explanation
1	Fresh
2	Young
3	Mature
4	Old

The above age classification was implemented on Moon River I by WNRE, Inc. The classification on Moon River II was not only applied to craters less than 50 meters in diameter, but also, to those craters greater than 50 meters. The distinguishing feature between greater than and less than 50 meter craters is that those craters of less than 50 meters will not have a slope and soil class associated with them. Additional information can be found in Table II.

b. Density of Lineal Features

The rationale for encoding lineal features was that if the line, representing lineal features present on the geologic map, extended more than half way across (North/South and/or East/West) a specific grid square, that grid square would be encoded as presenting a challenge to mobility. The codes used were:

Code	Explanation
0	If no lineal features present
2	If lineal features are present which would create a challenge.

c. Block Count

The block count simply consisted of the number of blocks, down to resolution size, that were present within any grid square.

2.2 Vehicle Inputs

In addition to terrain inputs, as abstracted from maps and photographs, it was necessary to quantify the characteristics of a typical Manned Lunar Rovin Vehicle so that its dimensions and performance characteristics could be compared with terrain demands. Relevant vehicle parameters are tabulated in Table III.

TABLE III

LUNAR VEHICLE DATA FOR LOCOMOTION ANALYSIS

Overall length	122 in.	
Overall width	77 in	
Wheel diameter	32 in	
Wheel base (center of axle to center of axle)	90 in	
Wheel width(center of wheel to center of wheel)	72 in	
Tread	9 in	
Clearance at full payload	14 in	
Step obstacle capability	30 cm at μ = 0.6*	
Crevice capability	70 cm at μ = 0.6	
Minimum turning radius wall to wall (front and rear Ackermann)	122 in	
Angle of approach	35 deg	
Angle of departure	90 deg	
Slope capability (hard ground)	25 deg	
Wheel spring rate, front	32 lb/in.	Rear 32 lb/in
Net vehicle mass	465 lbm	
Gross vehicle mass	1370 lbm	
Weight distribution	45% front,	55% rear (nominal CG)
Front Suspension Spring Rate	14 lbs/in	(0-9 in)
Rear Suspension Spring Rate	14 lbs/in	(0-9 in)
all wheels:	500 lbs/in	(0-9 in)

* μ = coefficient of friction

Table III (Cont.)

Vehicle can climb a 25° slope (hard surface $\mu = .6$)	
Power source:	2 independent silver zinc batteries provide 8712 watt-hrs. These batteries can be discharged to 90% capability before recharge. The power is allocated at 7,112 watt-hrs. for mobility and 1600 watt-hrs as a useful power source for other items as TV camera, communication, etc. if their own separate power sources should fail.
Maximum continuous-duty wheel torque	78 ft-lb at 35 rpm wheel speed
Maximum wheel speed	118 rpm at 5 ft-lb wheel torque
Nominal CG	32" from ground
Suspended Mass	1274 lbs
Wheel Mass	24 lbs
Wheel Damping Rate	2.5 lbs/ft/sec
Vehicle pitch moment of inertia	283.65 slug-ft^2
Wheel rotational moment of inertia	2.2 slug-ft^2
Vertical damping rate	17.3 lbs-sec^2/ft
Horizontal suspension rate	51,000 lbs/ft
Horizontal suspension damping rate	2420 lb/ft/sec

3. EVALUATION MODEL CONSIDERATIONS

Aside from the accuracy of lunar terrain input data, the most important consideration in the preparation of trafficability and visibility maps is the validity of the mathematical models employed. In the following two sections, general descriptions of the trafficability and masking models are presented. More detailed information is given in Appendix I and Appendix II.

3.1 Trafficability Model

The basic vehicle-terrain interaction model for trafficability was developed by WNRE, Inc.[5] Digitized map information, in which each 50-meter square in the area is assigned codes denoting vehicle challenges, is provided from several map sources. These sources are converged, so that with each grid square there is associated a vector or collection of code values which completely define that portion of the terrain as far as its relevance to the vehicle model is concerned. In a given region of terrain, the number of distinct possibilities is limited and is usually much smaller than the number of grid squares. Each distinct collection of code values is called a unit terrain and represents a specific challenge to the vehicle.

Each unit terrain can be evaluated for its compatibility with the vehicle independently of where that unit terrain occurs on the lunar surface. The outcome of this evaluation is that the unit terrain codes are transformed into a trafficability performance code, as shown in Figure 4. This code denotes one of four states: Go, No-Go, Troublesome, and Very Dangerous. The Go category is assigned when the unit terrain is such that no feature of the terrain is serious enough to prevent negotiation of the area involved. In the event of

---

(5) W.C. Grenke and C.J. Nuttall, Jr., op. cit.

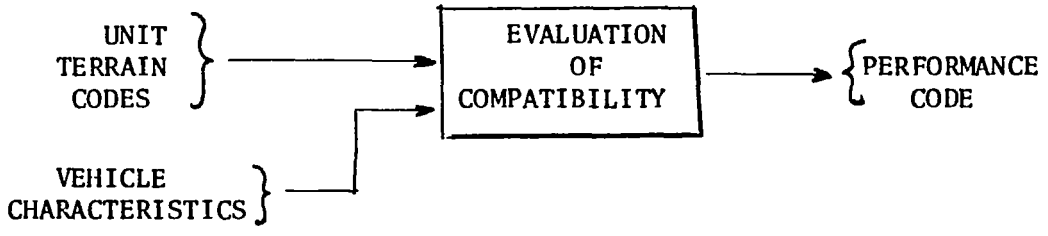

FIGURE 4

PROCESSING OF UNIT TERRAINS

No-Go, obstacles or terrain features are present which would immobilize the vehicle. The other two categories are conditional Go conditions. In the troublesome category, it might be necessary to back up and make a second try at the terrain, but it is presumed that the vehicle could be recovered. In the case of the Very Dangerous category, however, there is appreciable risk that the vehicle might be stopped under conditions from which it would be impossible to recover for a second try.

The processing of unit terrains is accomplished by subjecting each to a series of "tests", as listed in Table IV.

TABLE IV.

PERFORMANCE TESTS OF VEHICLE-TERRAIN COMPATIBILITY

Test	Failure Mode
A	Density of lineal features
B	Mean spacing of resolvable blocks ($\geq$ 2m)
C	Mean spacing of all nonnegotiable blocks
D	Mean spacing of 20-50 meter craters
E	Mean spacing of 5-20 meter craters
F	Approach interference
G	Departure Interference
H	Belly clearance
I	Joint clearance
J	Pitch stability
K	Roll stability
L	Net traction
M	Available torque

Details of these tests are given by Grenke and Nuttall (op.cit.) and will not be repeated here.* A typical example will suffice to illustrate the implementation of the scheme. For example, in Test K, Roll Stability, failure occurs if the terrain slope is such that it exceeds the maximum which could be tolerated without the vehicle overturning. Quite clearly, all applicable tests must be passed if the vehicle is to operate successfully in a grid square to which the particular unit terrain applies.

Once a performance code has been assigned to each of the unit terrains, these codes must be distributed in the plane of the map in one-to-one correspondence with the occurrence of the unit terrains in the grid squares. This plotting operation is accomplished by substituting the applicable performance code for each unit terrain code, wherever that code occurs in the digitized array of grid squares.

Further information can be provided in the trafficability map by assigning to each unit terrain a measure of the energy required to negotiate one kilometer of path length. Again, the rationale for this calculation is available in the work of Grenke and Nuttall (op.cit). If all Go/No-Go tests were successfully completed, the energy consumption can be computed and can be thresholded into intervals. For example, one unit terrain might be classed in the interval 50-99 watt-hrs/kM, whereas another unit terrain might be classed in the interval 100-149 watt-hrs/kM. By assigning a discrete code to the intervals, a map can be presented which subclassifies all Go areas into categories denoting differing levels of energy consumption. Another possibility, and one used extensively in this report, is to present energy codes for all map areas which are unconditional Go, but, in the case of Troublesome or Very Dangerous areas, to override the energy codes by the applicable trafficability codes.

For further detail on the analysis of energy expended in traversing the lunar terrain, refer to Appendix III.

---

* Note: Not all of the tests are applicable to the Manned Rover. For example, some apply only to a 6 x 6 vehicle.

3.2 Visibility Model

Point-to-point visibility on the lunar surface was analyzed by means of a computer model called ASTERISK. In effect, the model performs a "search" from a selected observation point to every other grid point in the plane. For example, consider Figure 5.

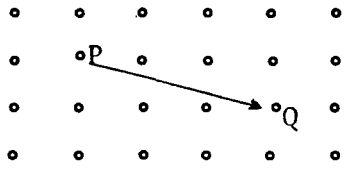

FIGURE 5
LINE-OF-SIGHT "SEARCH" PROCEDURE

Here P is the observation point and the specific point being interrogated for visibility is the point Q. If any elevation along PQ is high enough to interrupt the line of sight, then the point Q is said to be "masked" by intervening terrain. Since elevations are tabulated only at the grid points, it is often necessary to interpolate elevations along the sighting path.

The computer output takes the form of an array of asterisks and blank spaces. One or the other of these symbols is assigned to each grid square in the digitized array. Asterisks denote that a given point in the array is masked from view from the observation point; a blank denotes that visibility exists.

4. OUTPUT CONSIDERATIONS

In all cases in which a computer model was used to develop map information, the output of the model took the form of a computer print-out consisting of an array of symbols. These symbols were trafficability codes and energy-consumption levels in the case of the trafficability model. In the case of the visibility model, the symbols denoted masked or unmasked areas.

For maximum ease of interpretation, it was found advantageous to hand sketch the computer print-out in order to effect three important improvements.

First, the raw data print-out is distorted in dimensions, because the space between lines of print is greater than the distance between symbols within a line. By introducing appropriate scale changes in the sketching process, this distortion can be eliminated.

Second, the computer print-out, albeit meaningful, is still only an array of symbols and hardly resembles the maps to which one is accustomed. Sketching can be thought of as an "inverse digitization" which transforms a digital array back into the continuous form characterizing the usual cartographic product.

Finally, a certain amount of editing and geographic judgment is often in order in the interpretation of a computer-generated map. In transforming the computer print-out into the more conventional map form, the cartographer can override minor discrepancies or can introduce the degree of geographic generalization appropriate to the problem under study. Thus the production of the final trafficability or visibility map can be regarded as a "computer-aided" process rather than as a fully automated one. In particular, many questions of map design can be resolved in this way, and maps can be produced having a more nearly maximum appeal from the standpoint of ease of reading and interpretation. In the work performed under this program, it was found that transparent overlays produced from the computer printouts were particularly useful. When placed over the appropriate base map, the constraints of the terrain on trafficability and visibility can be readily appreciated, and positional reference can be greatly aided.

5. RESULTS

The results of our analysis and mapping of the Fra Mauro site fall into three general categories: (1) trafficability mapping, (2) visibility mapping, and (3) horizon representation.

5.1 Trafficability Maps

Trafficability maps were prepared for a region on the moon's surface having dimensions of approximately 3.5 kM by 4 kM. The area mapped is indicated in Figure 6 in relation to Cone Crater, Triplet Crater and other evident features of the Fra Mauro base map.

The computer print-out of the trafficability map is shown in Figure 7. On this map, blank spaces denote untrafficable areas, T denotes troublesome areas, and V denotes areas which are very dangerous. Except for areas occupied by question marks, all other areas denote Go conditions but are occupied by a numerical code which indicates energy requirements per kilometer of path traversed. The regions occupied by question marks indicate that in those regions some important item of input information was not available and that, consequently, it was not possible to generate the appropriate trafficability codes. Also, in a few isolated instances, the range of input data apparently exceeded the applicable range of terrain parameters allowed by the WNRE, Inc. traction model. Such instances occurred in only a few of the unit terrains, and these terrain types occurred only very rarely. Moreover, these terrain types were usually very severe and would normally be rejected on other bases.

Figure 8 (p. 27) is the GO/NO-GO reference map. Figure 8 (p. 27a) is with overlay superimposed showing rectified, hand-sketched GO/NO-GO map. Two other maps are shown with overlays superimposed (pp. 27b, 27c) as developments of two separate ranges of energy consumption. Thus if one wishes to observe how trafficability area is restricted by energy demands, in addition to trafficability hazards, these overlayed maps can be used. By superimposing the first overlay (p. 27b), the trafficable area is restricted to that not requiring more than 149 watt-hr/kM of energy; by superimposing both overlays (p. 27c), the trafficable area is restricted to that not requiring more than 199 watt-hr/kM of energy.

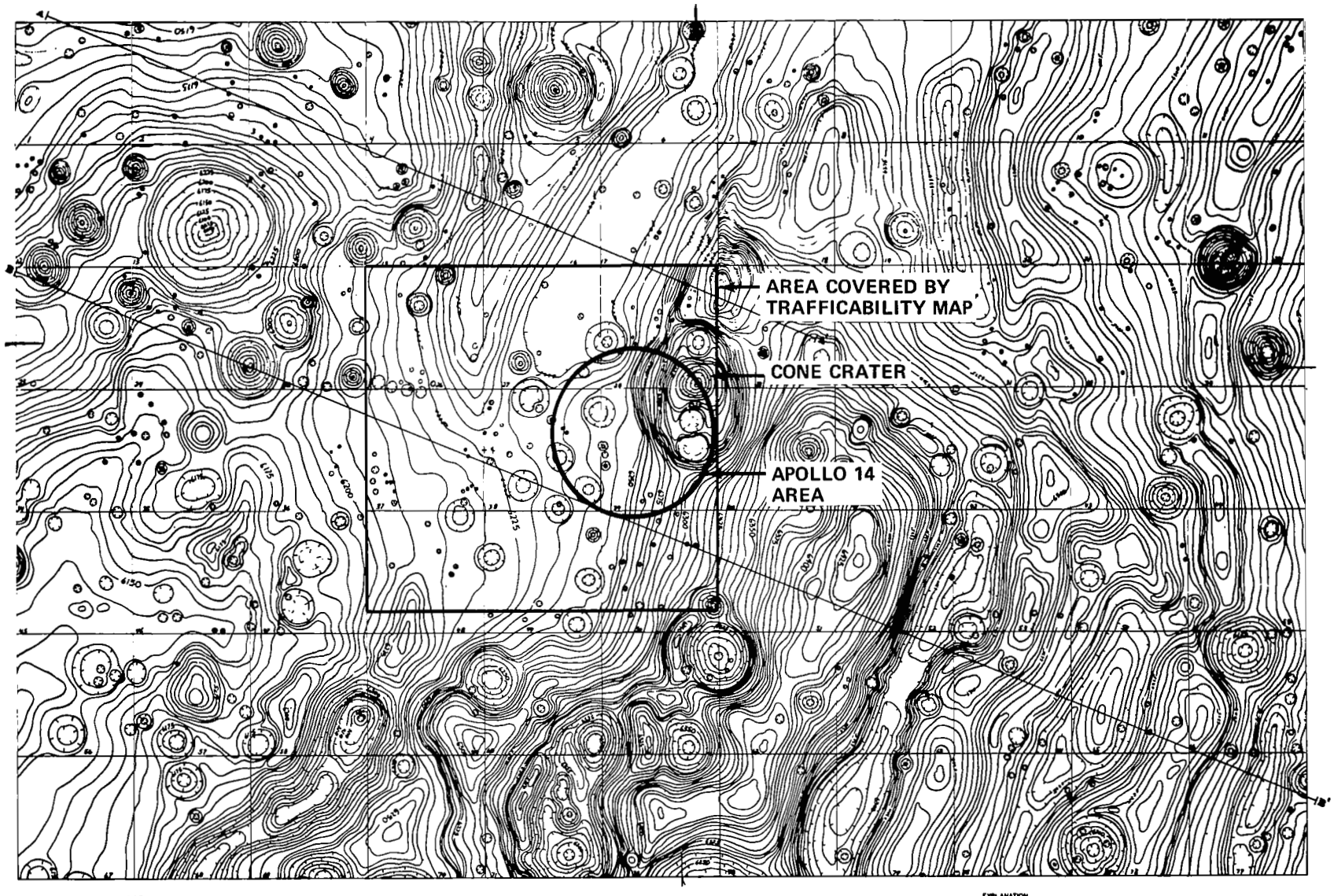

Figure 6 AREA MAPPED FOR TRAFFICABILITY

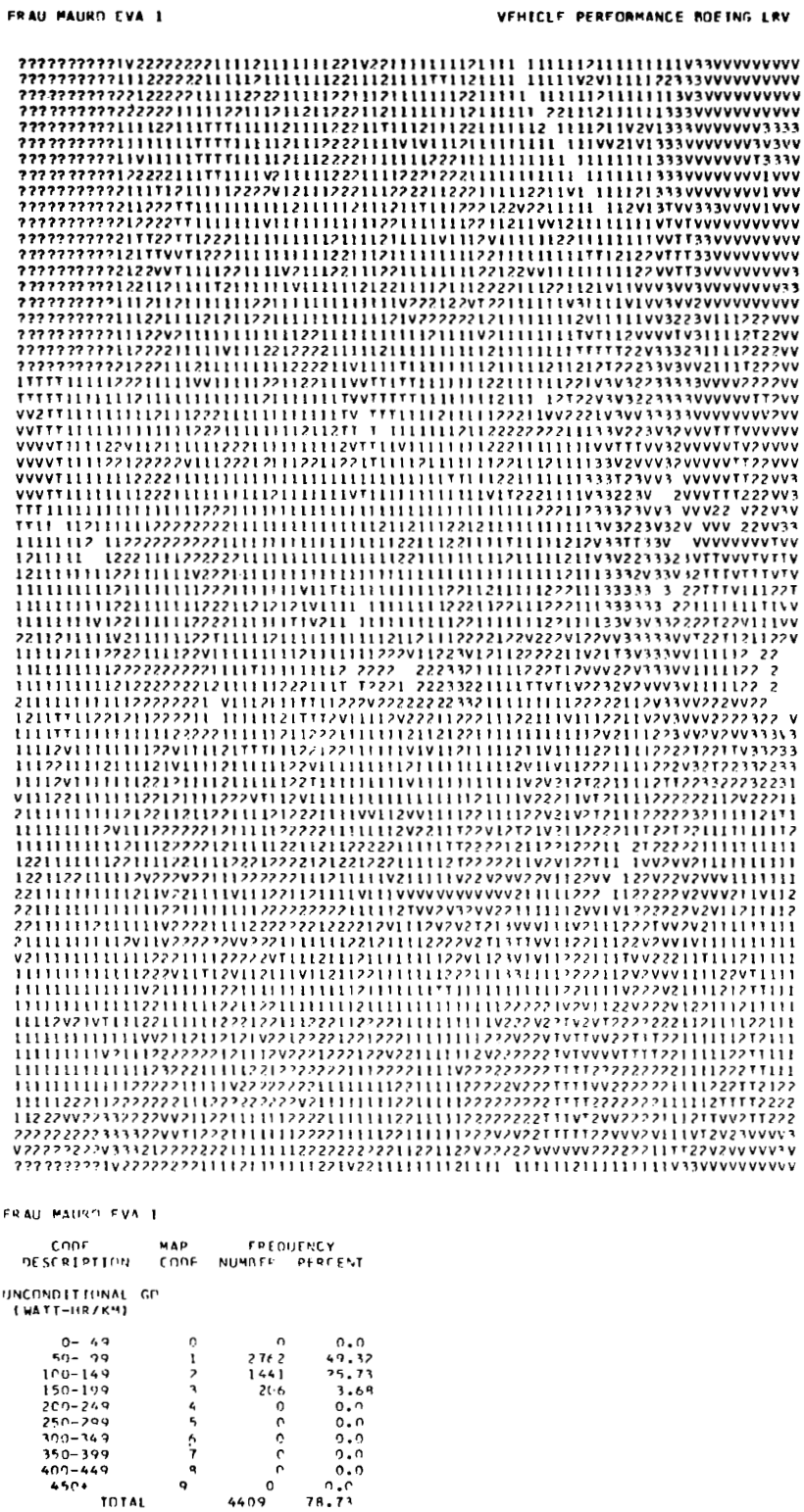

Figure 7 COMPUTER PRINT-OUT OF TRAFFICABILITY MAP

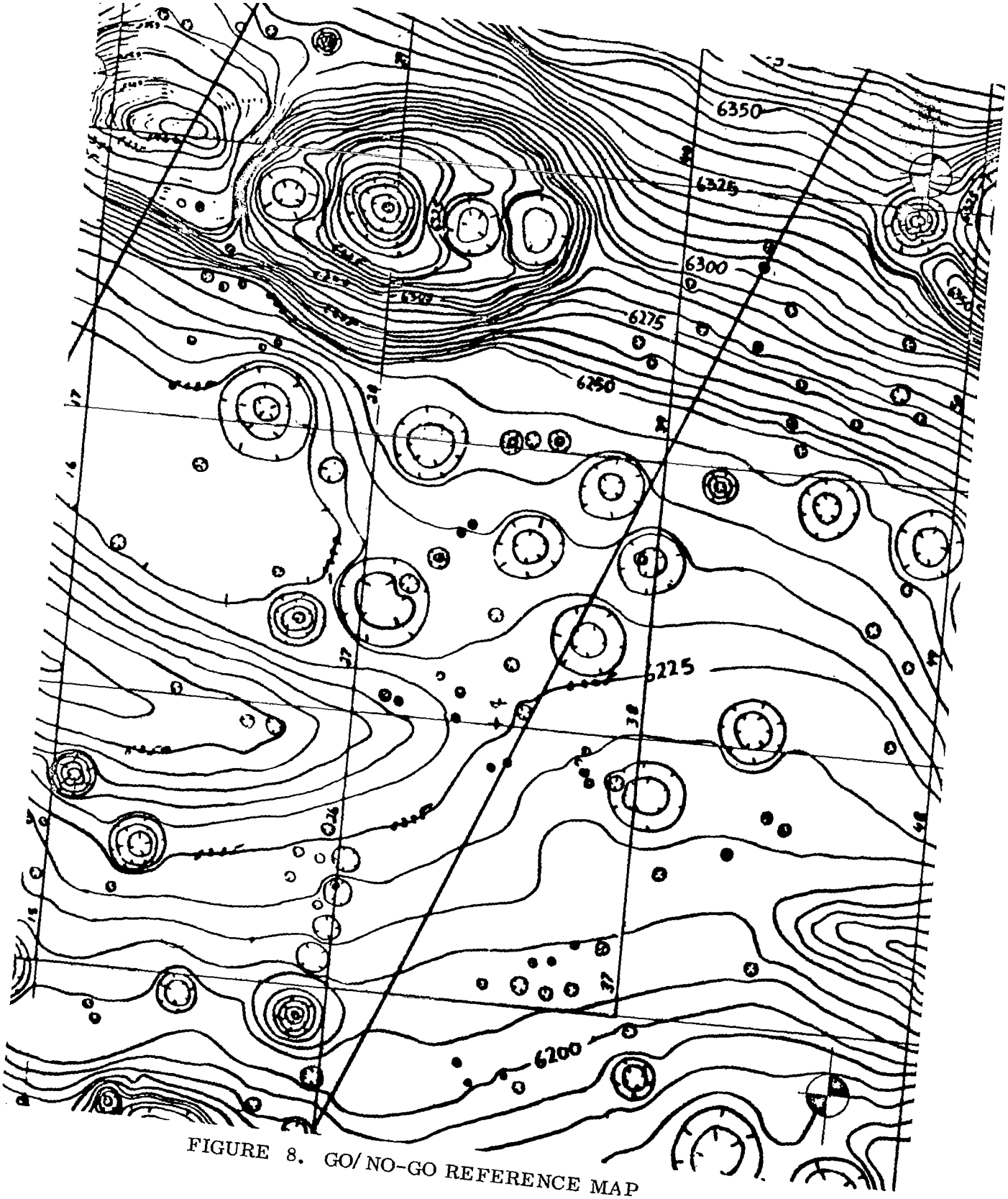

FIGURE 8. GO/NO-GO REFERENCE MAP

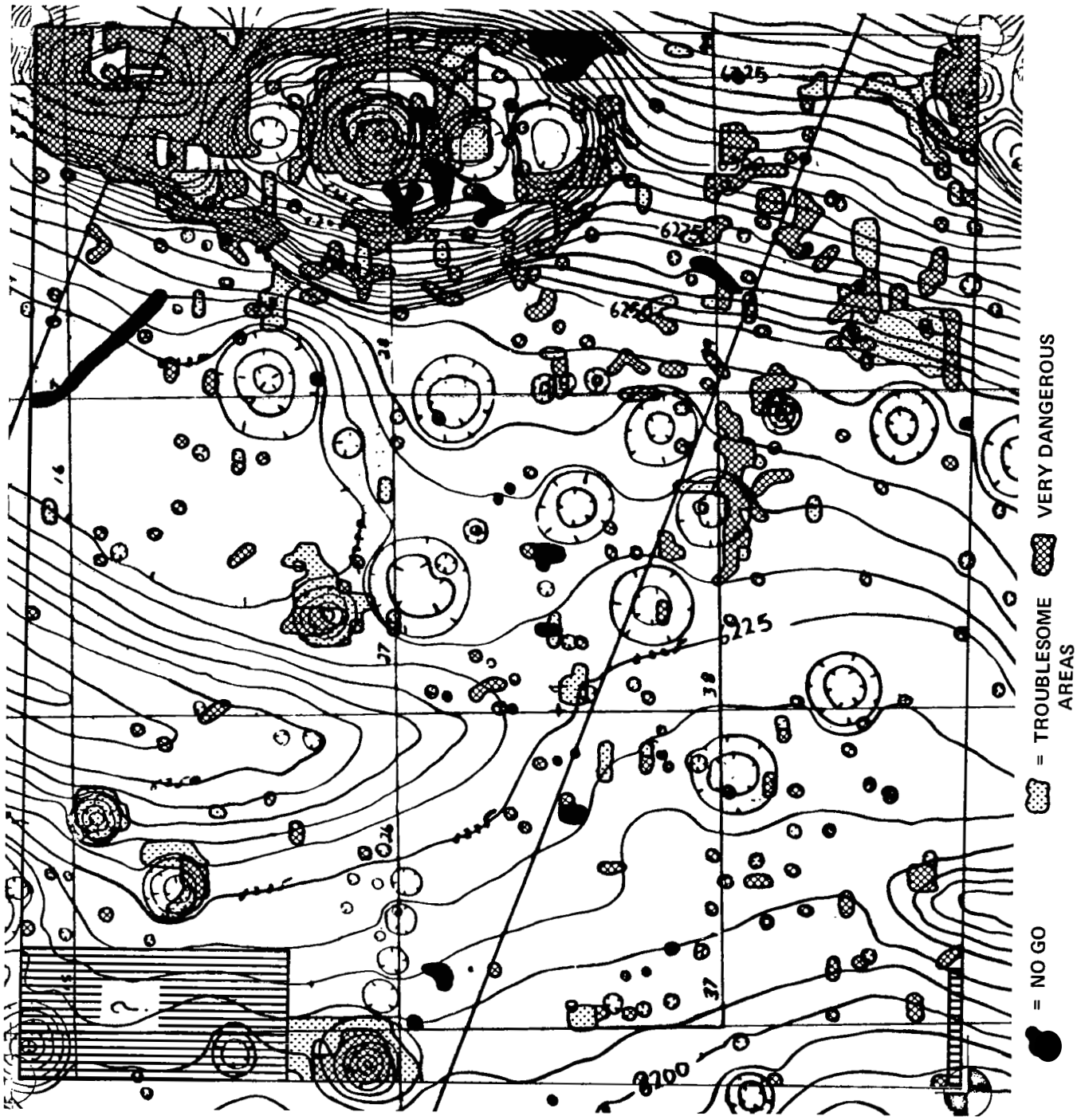

FIGURE 8. GO/ NO-GO MAP (With Overlay)

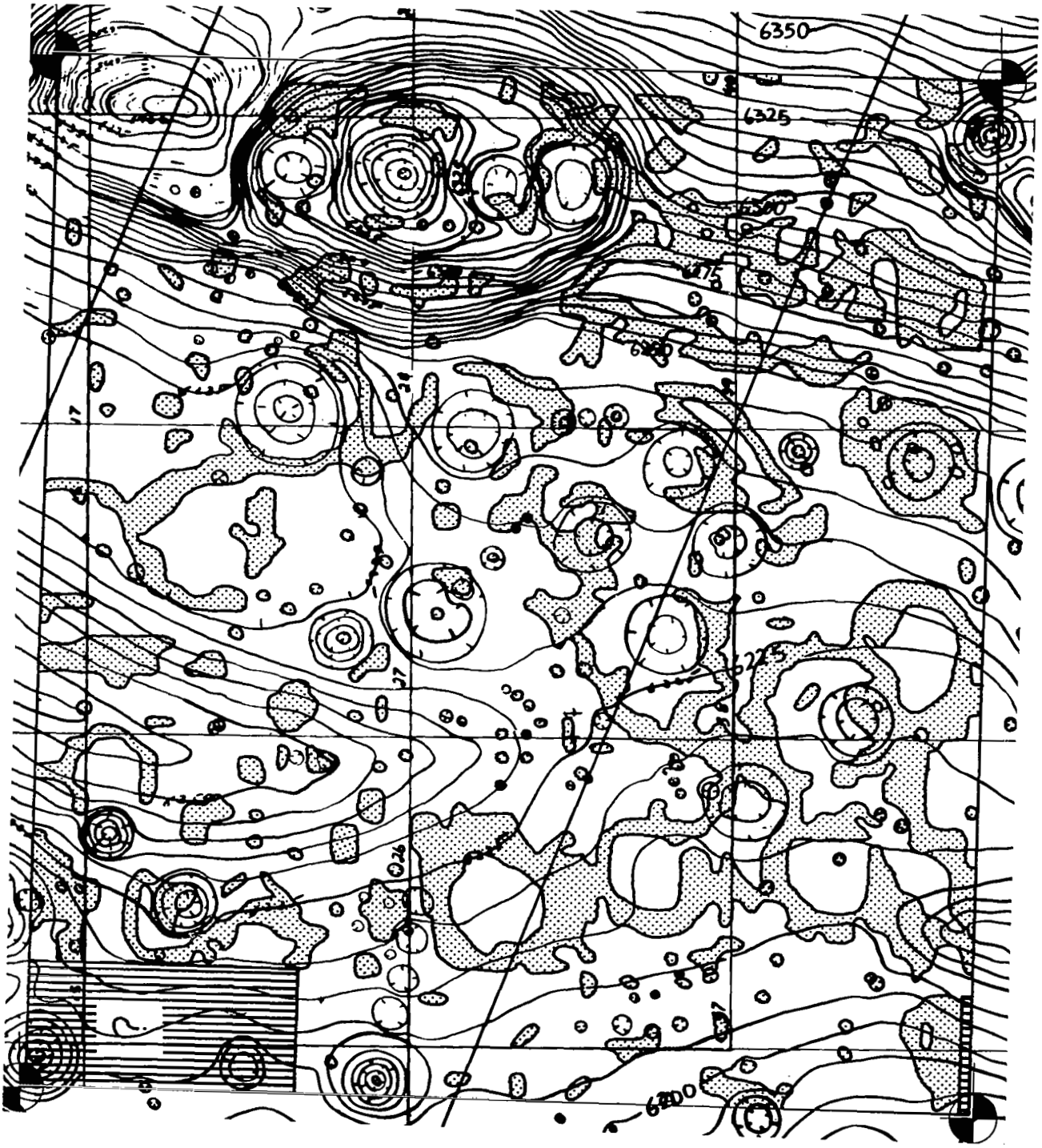

FIGURE 8. GO/ NO-GO MAP (With Overlay)

100 - 149 WATT - HR/KM

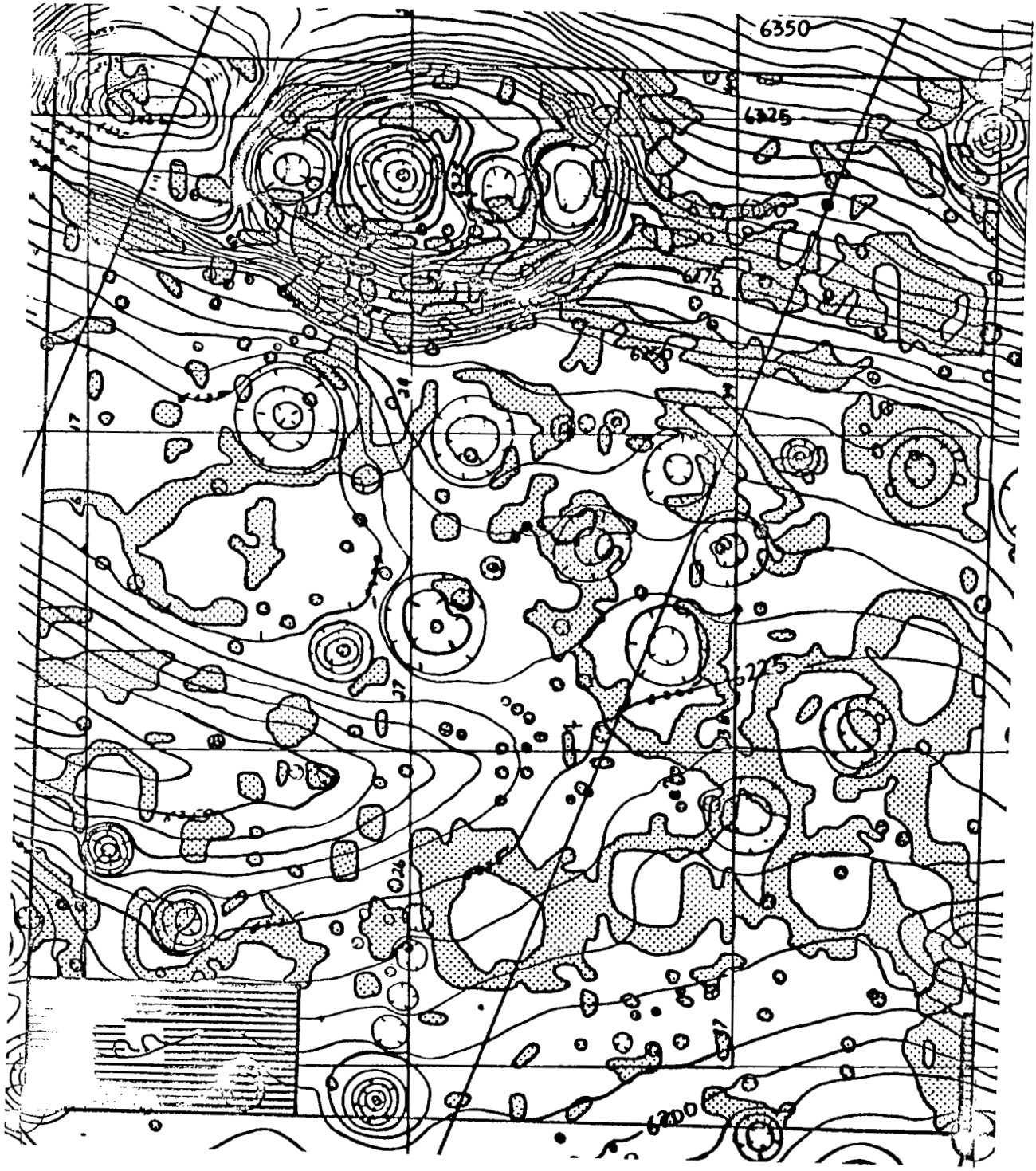

FIGURE 8. GO/NO-GO MAP (With both overlays)

5.2 Visibility Maps

Visibility maps were prepared for three terrain landmarks and for the lunar module located at an assumed touch-down point.

The landmark visibility maps are shown as computer print-outs in Figures 9, 10, and 11. In connection with these maps, a word of explanation is in order. In particular, it will be noted that the print-outs contain not only asterisks and blank spaces but arrays of zeros and ones as well. The configuration of the 0 and 1 digits delineates what we have elected to call the "landmark feature" of interest. The configuration of the 0 digits delineates that part of the landmark feature which protrudes above a certain elevation selected as a truncation plane. By sighting at this elevation and performing the visibility analysis accordingly, one is assured that all parts of the landmark above the truncation plane would be visible. In practice, the elevation of the truncation plane should be chosen so that a sufficient amount of the landmark feature is visible to facilitate recognition of the landmark. The 1 digits represent part of the surrounding terrain which was manually analyzed as a preprocessing step prior to computer analysis of the remaining terrain surrounding the landmark feature. A 1 digit denotes visibility and, on the subsequent hand-sketched maps, areas occupied by the 1 code become unshaded (unmasked) areas.

The hand-sketched maps are presented with the transparencies superimposed on the corresponding base map in Figure 12. Unshaded areas on either of the maps represent positions from which the particular landmark should be visible. If two of the transparencies are employed simultaneously, unshaded areas represent positions from which <u>both</u> landmarks are visible. If all three transparencies are employed, unshaded areas denote positions from which all three landmarks should be visible. Shaded areas may denote that one, two or all three landmarks are masked, depending on which of the overlays produce the shading.

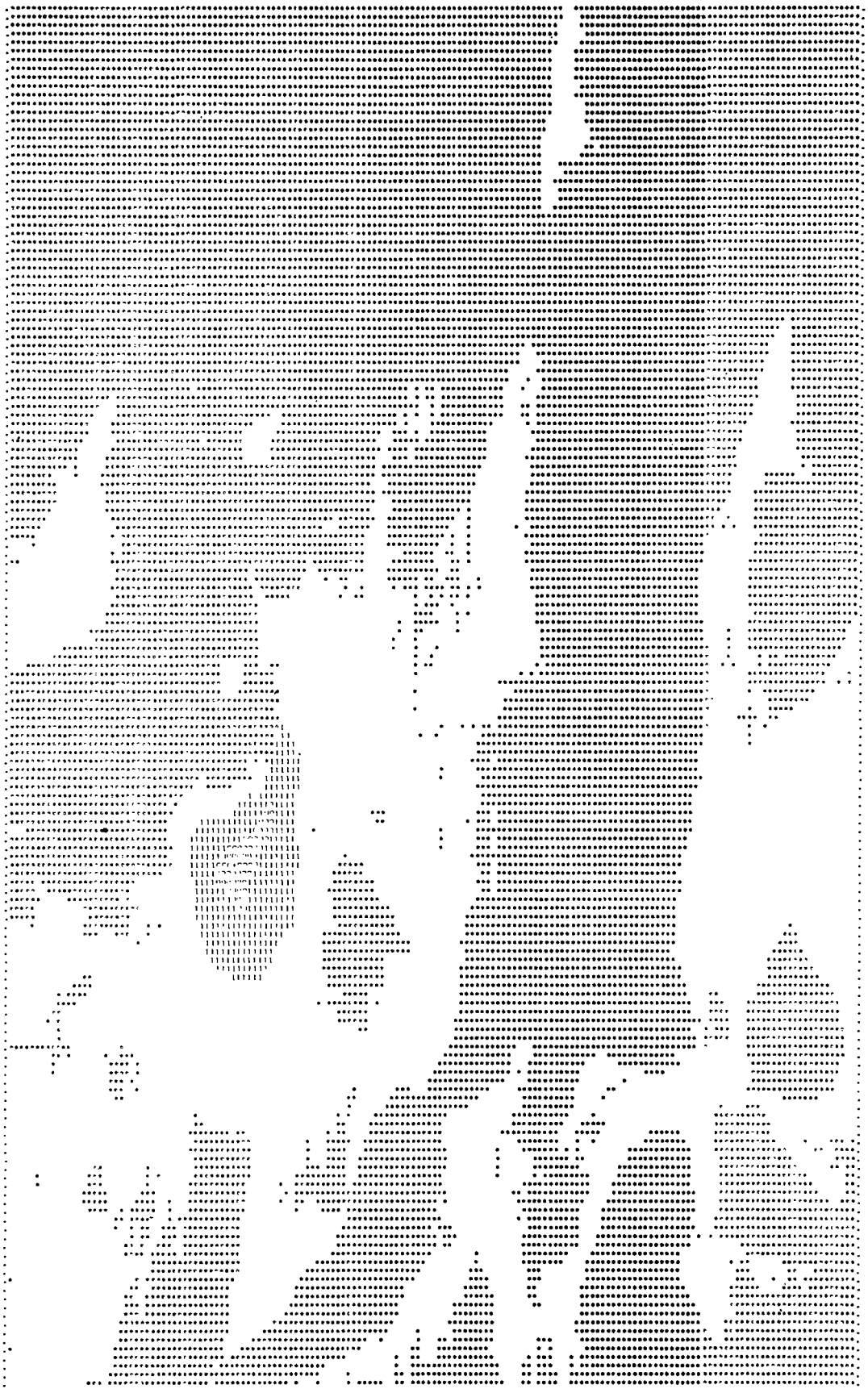

Figure 9 COMPUTER PRINT-OUT OF VISIBILITY MAP

ITY MAP

Figure 11 COMPUTER PRINT-PUT OF VISIBILITY MAP

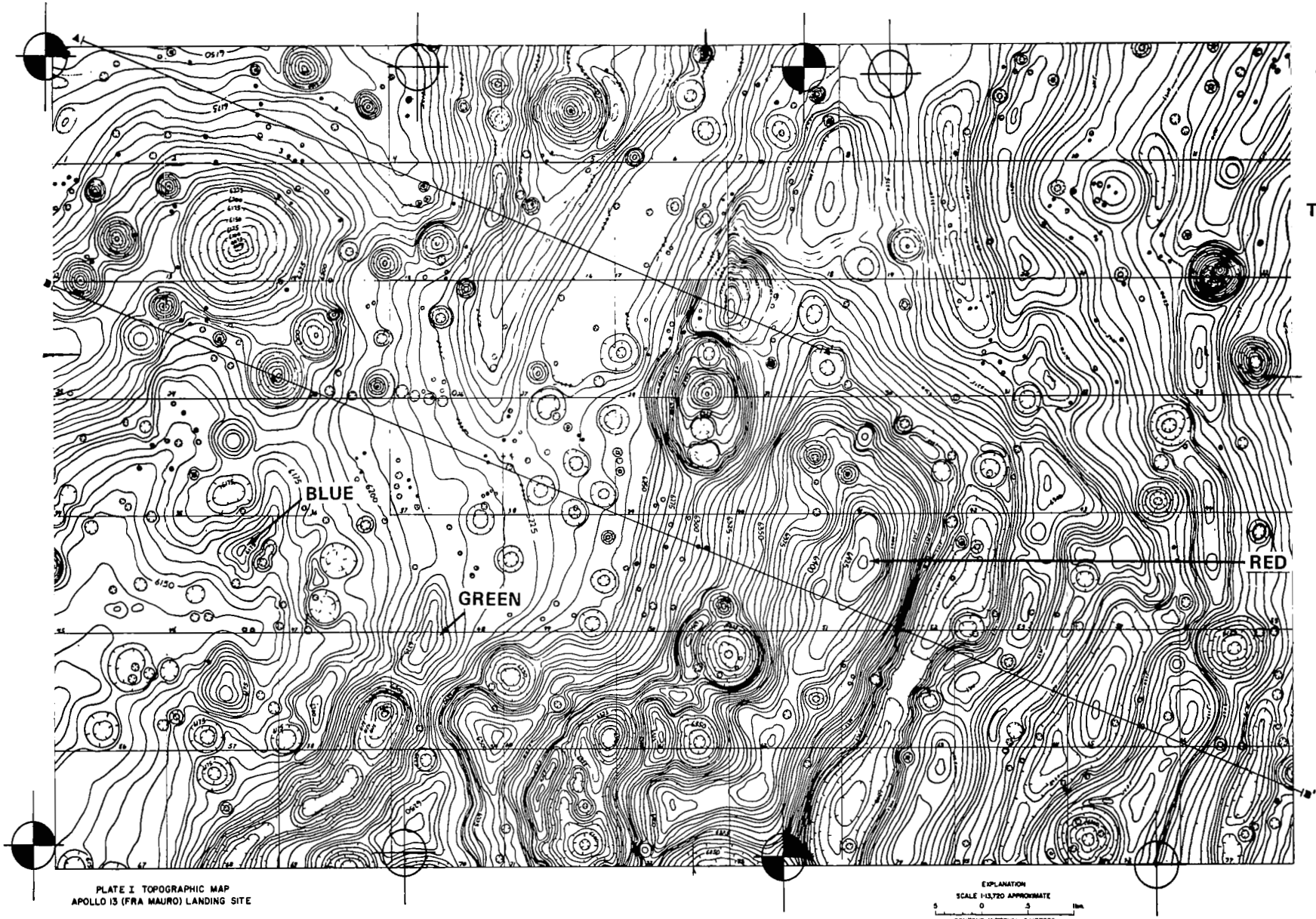

FIGURE 12. VISIBILITY MAP WITH LANDMARKS (Blue, Green, Red)

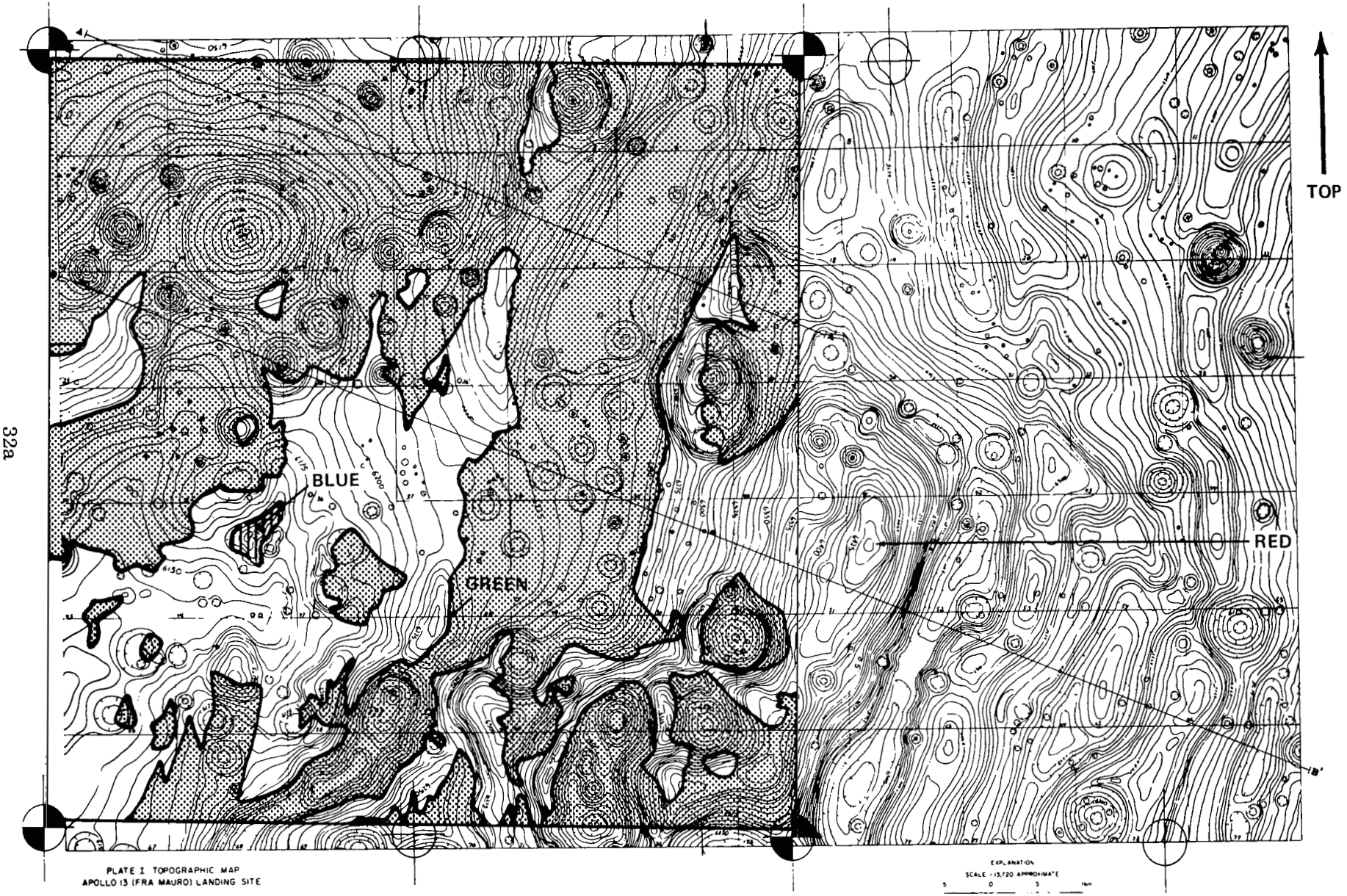

FIGURE 12. (Continued) OVERLAY SUPERIMPOSED TO SHOW VISIBILITY OF BLUE LANDMARK

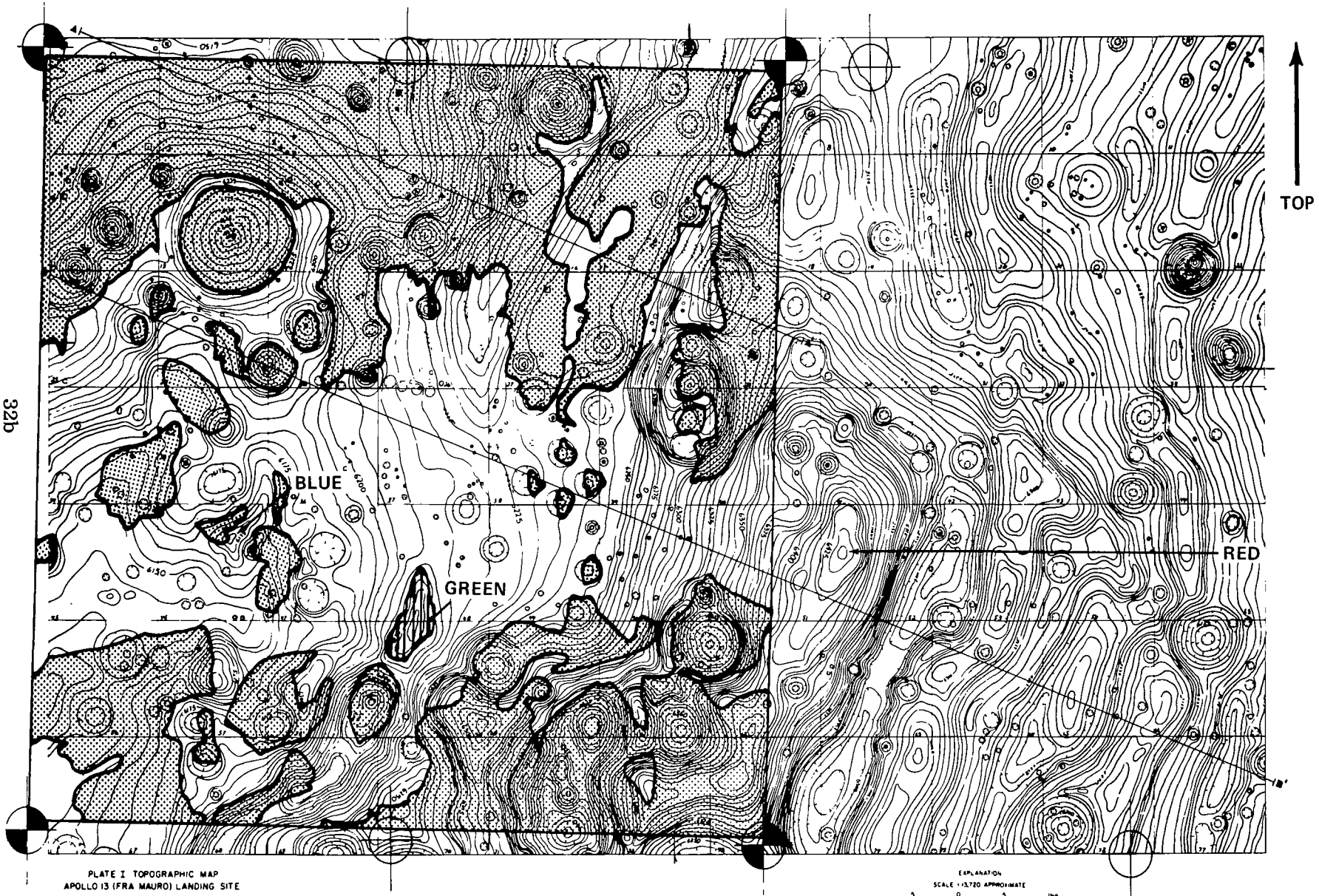

FIGURE 12. (Continued) OVERLAY SUPERIMPOSED TO SHOW VISIBILITY OF GREEN LANDMARK

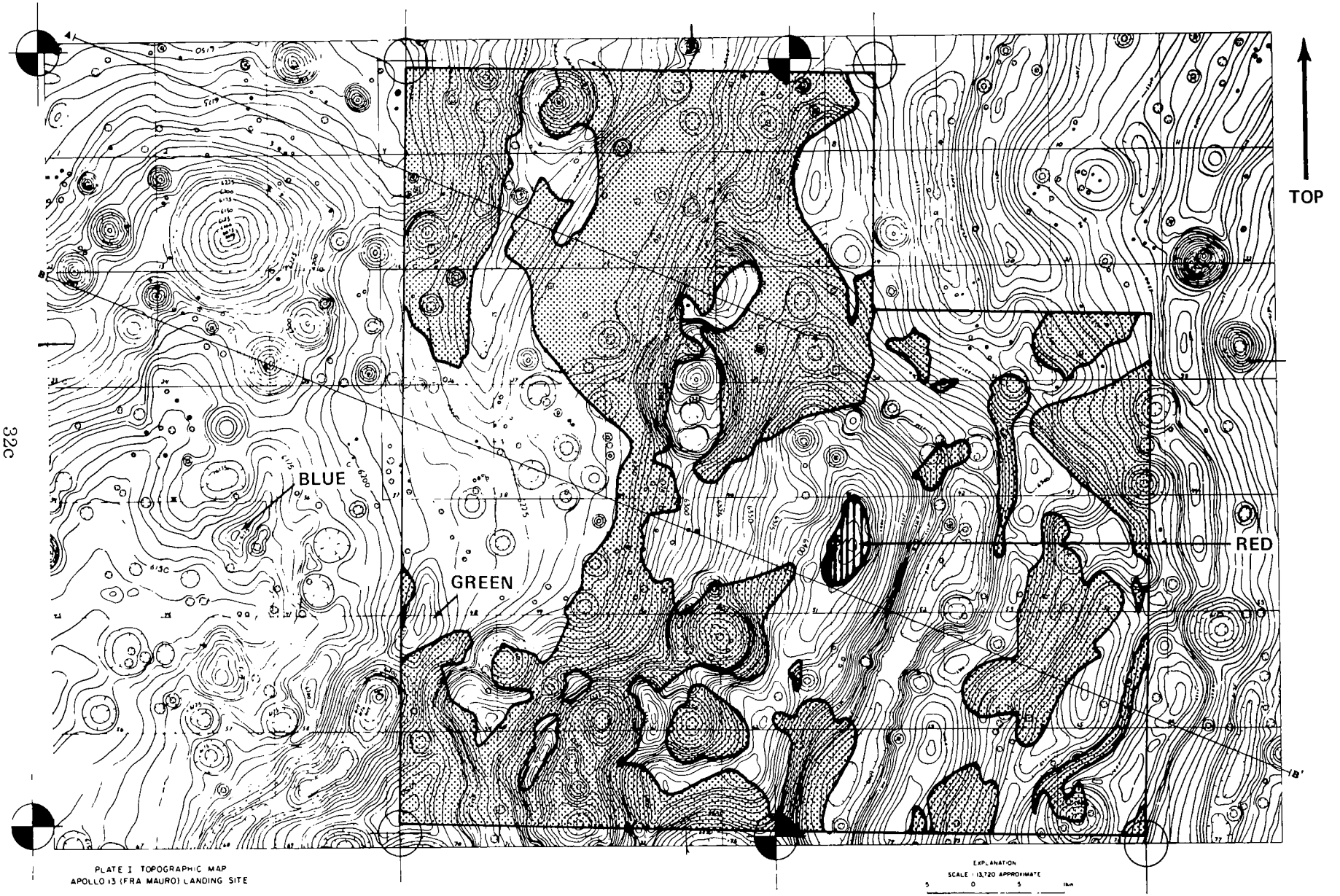

FIGURE 12. (Continued) OVERLAY SUPERIMPOSED TO SHOW VISIBILITY OF RED LANDMARK

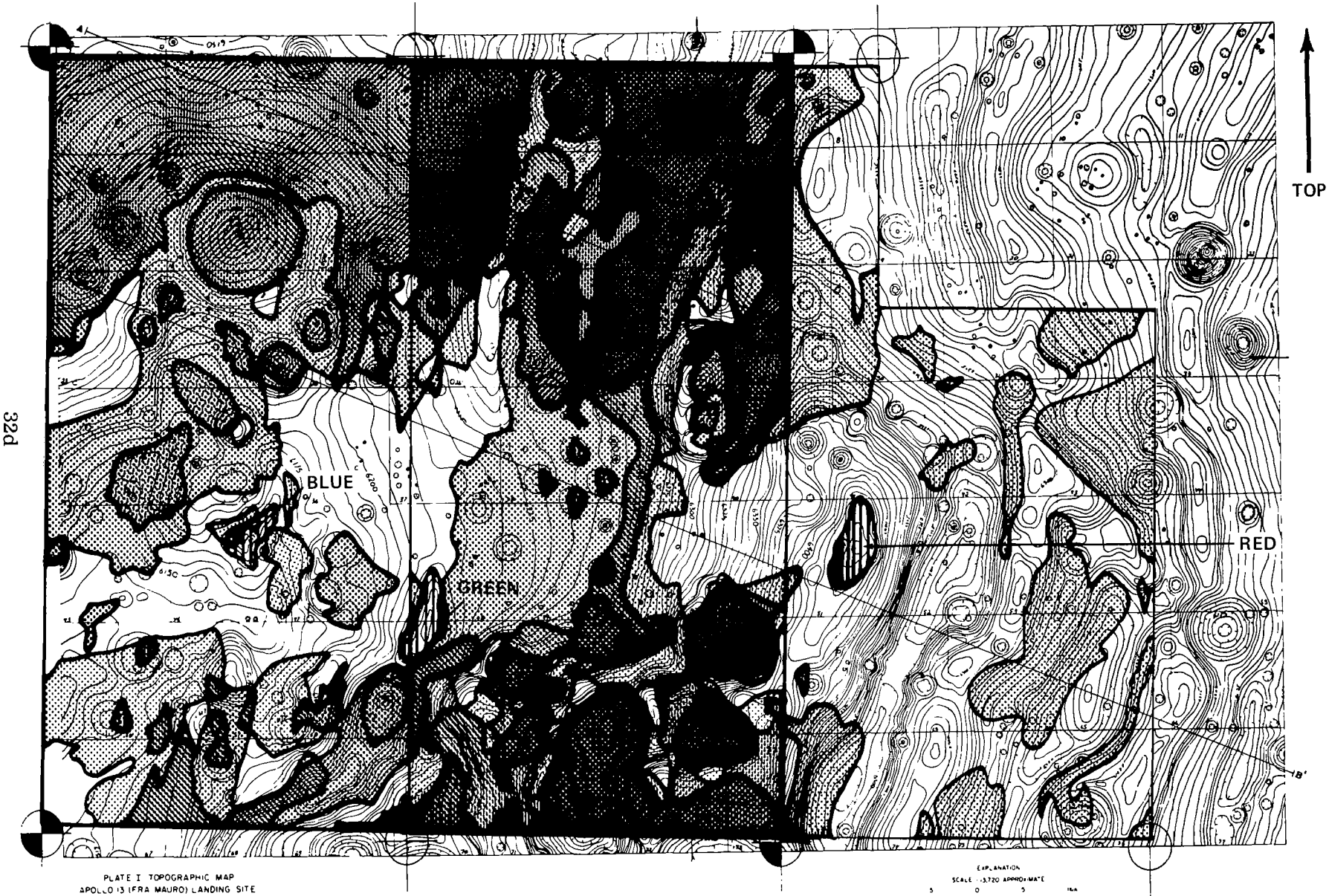

FIGURE 12. (Concluded) OVERLAYS (Blue, Green, and Red) SUPERIMPOSED SHOWING REMAINING AREA IN WHICH ALL LANDMARKS ARE VISIBLE

In checking out the visibility model, the lunar module was employed as a landmark in several occasions. Of particular interest is Figure 13, a computer print-out of a visibility map for the module positioned at the presumed touch-down point on the moon. This map, as hand-sketched, is shown in Figure 14 as a superimposed overlay on the appropriate base map. The sighting point for the module is chosen as 7 meters above the ground, thus assuring that an appreciable part of the module would be visible. The coverage of the map is sufficient to include the EVA traverses planned for the Apollo 14 mission.

As shown in Appendix II, it was a visibility map of the lunar module that first called to our attention the need for terrain smoothing. This smoothing was necessary to prevent spurious masking by the "terraces" produced as artifacts of the digitization process.

5.3 Horizon Graphics

In visualizing the horizon as viewed from a particular point, one must keep in mind that distance to the horizon is determined in part by the curvature of the moon and in part by the elevation of lunar features. Furthermore, the features which constitute the horizon appear at different ranges from the observer as he looks in various directions. In the study undertaken under this project, the horizon offered few features which would provide help in identification of position on the moon. For more rugged terrain, however, it is expected that a profile or other graphic representing the horizon would be of considerable navigational use.

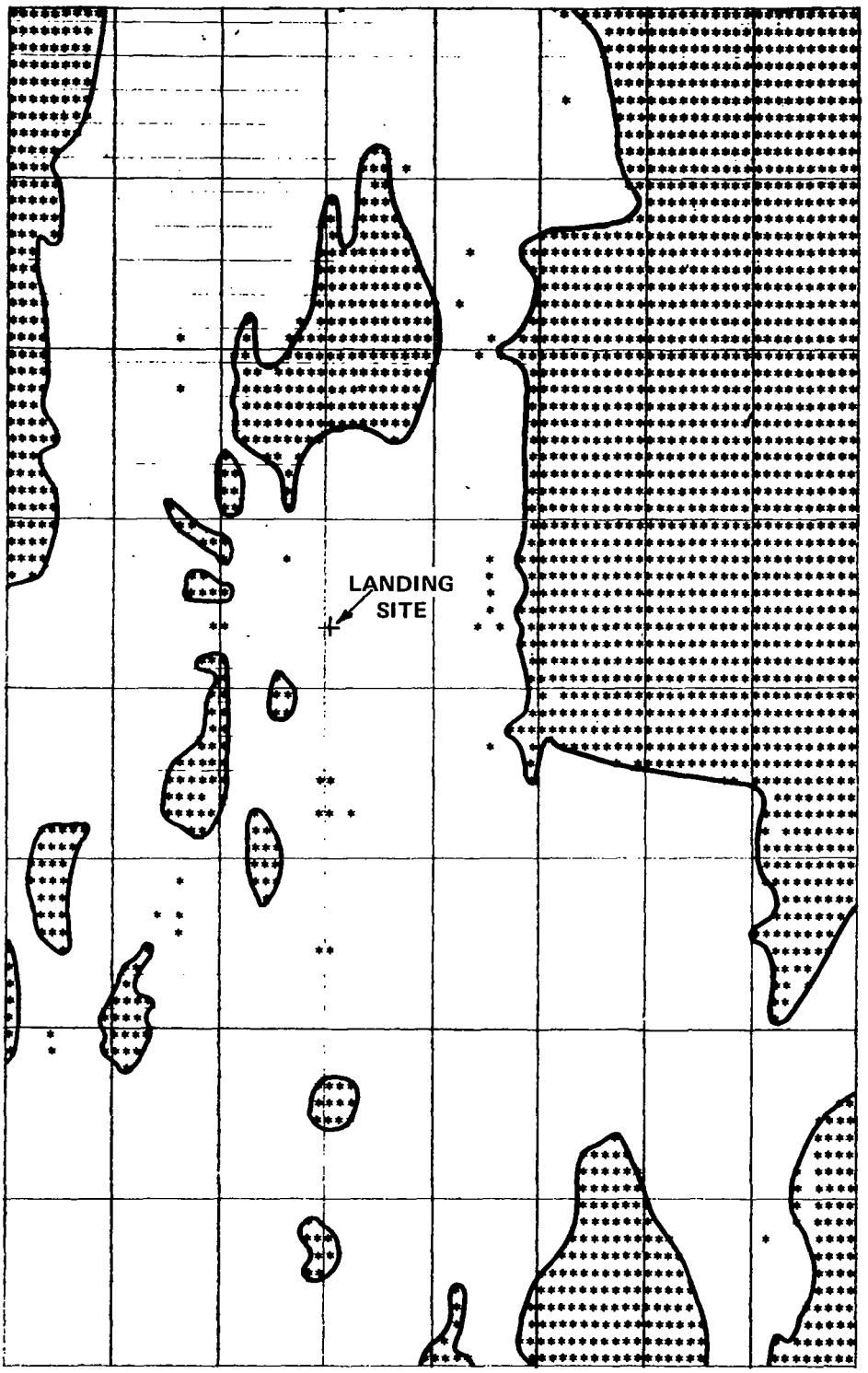

Figure 13 COMPUTER PRINT-OUT OF VISIBILITY MAP

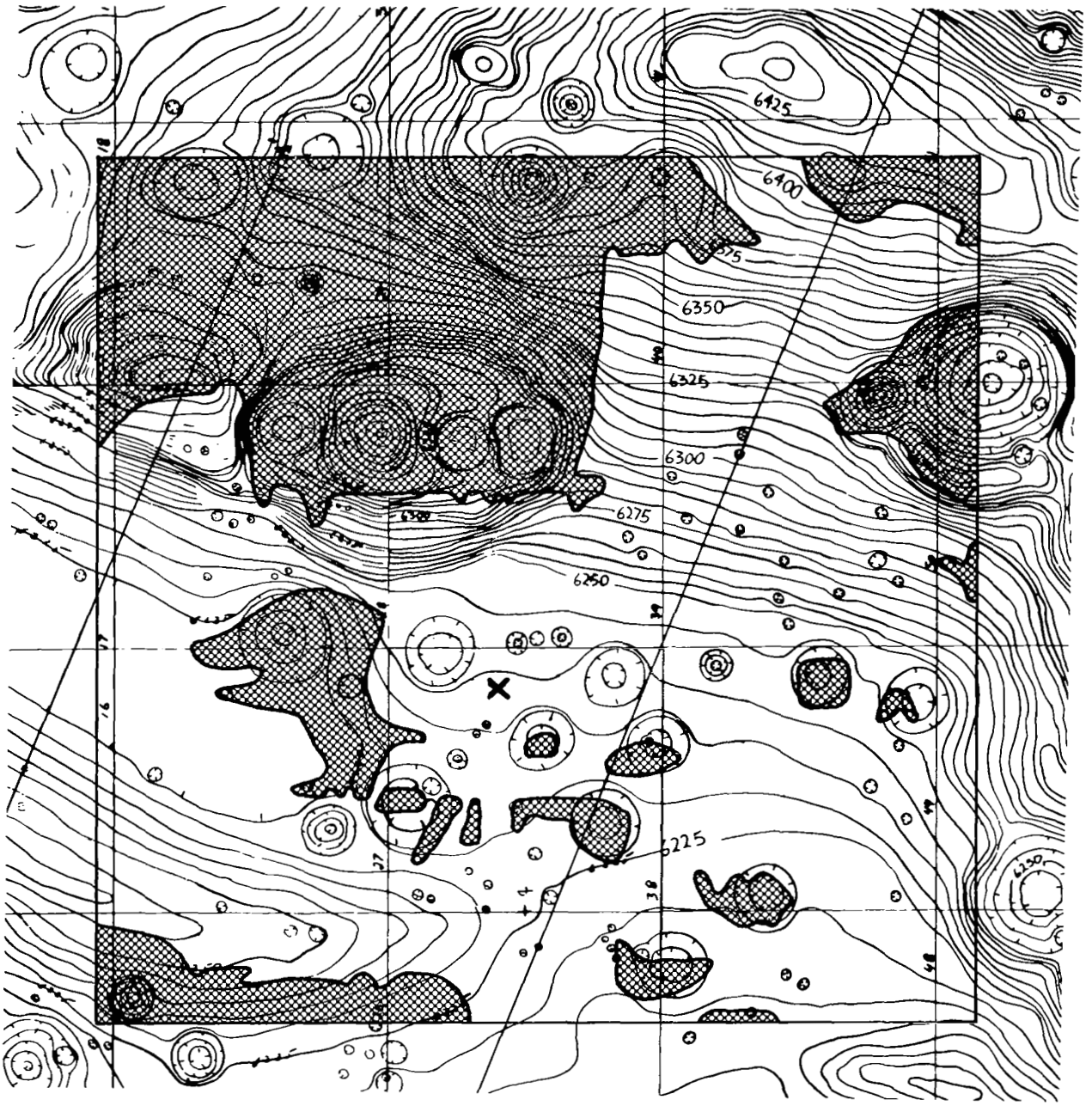

VISIBILITY FROM FRA MAURO LANDING SITE
X is the point at which visibility is determined

Figure 14 VISIBILITY MAP

6. CONCLUSIONS, RECOMMENDATIONS AND PROSPECTUS

Computer techniques for generating trafficability and visibility maps for the moon have been developed and successfully demonstrated on the Fra Mauro site of the Apollo 14 mission.

Difficulties were encountered in converging the various sources of lunar data to be used because the system of coordinates did not agree from one map to the other. For final coordination of the various sources of data, it was necessary to reference the observations to recognizable features, such as identified craters, which were common to the several data sources. For future work, it is recommended that considerable caution be exercised in the use and interpretation of map coordinates. For the type of detailed analysis represented by this report, it is believed advisable to develop a local system of coordinates which assures internal consistency among the various maps and photographs employed.

A second source of difficulty was encountered in digitizing the lunar elevations to be used subsequently in line-of-sight analysis. It is recommended that smoothing be used to develop a reconstructed lunar surface before attempting to perform masking studies.

The visibility of landmarks from various locations on the lunar surface can be mapped by means of the methods presented herein. However, it must be recognized that the source elevation map employed a 5-meter contour interval and that the viewing height above the terrain was taken as two meters. In view of the fact that the uncertainty in elevation is of comparable magnitude to the viewing height, it is evident that errors in elevation could often alter an unmasked region to a masked one and vice versa. The desirability of better input data is therefore evident.

For greatest utility for locating position, it is evident that the landmarks should be chosen at relatively close range. In the maps presented in this report, the landmarks are too widely dispersed and

at too great a distance from the operational area to be of maximum usefulness. A greater number of landmarks mapped at closer range would be preferable. However, if the terrain is sufficiently rugged, more distant landmarks would be quite useful. The choice of both number and placement of landmarks must, therefore, be adjusted to the particular terrain and mission involved.

Several directions for extension of concepts developed under this contract are indicated:

- Application of trafficability and visibility analysis of future missions, particularly those in which the terrain has great relief and is of highly variable nature.
- Modification of the ASTERISK line-of-sight model to permit computer-based generation of the horizon.
- Application of existing methods for surface representation to the generation of slope maps based on topographic contour maps.
- Incorporation of trafficability and visibility maps as part of an unmanned rover concept.

In addition, a considerable amount of further study could be made of the Fra Mauro location at relatively small cost, by virtue of the fact that digitized input information and computer models are available.

APPENDIX I

TRAFFICABILITY COMPUTER PROGRAM DOCUMENTATION

Figure I-1 is a flow chart showing the interrelation of inputs and outputs for the trafficability computer program. Data from the digitization of maps and photos are converged by means of a program which produces unit terrains. These unit terrains are then processed by means of the WNRE-CAL trafficability program to generate a trafficability map as a computer print-out.

1. Unit Terrain Creation Program

This program receives digitized inputs from geology, photographic and slope sources and performs a data intersection to build a unit terrain code for each map location. A histogram sort is then performed on the codes to produce a unit terrain deck. This deck consists of one card for each unit terrain code which actually appears, with the cards sorted in decreasing order of occurrence. The map of unit terrain codes is then written out on magnetic tape.

The unit terrain coding applied in this phase of the project is almost identical to the system used by WNRE in their report "Accessibility of Specific Areas on the Lunar Surface as a Function of LRV Mobility Design Parameters," June 1970, pp. 106. The major difference is that digit 7, "Crater wall angle" has been replaced by terrain gross slope. This gross slope is developed in the following manner:

(1) Gross slope is set equal to digitized slope value.

(2) If the terrain square is located within a crater greater than 50 meters in diameter, but less than or equal to 200 meters in diameter, the crater inner wall angle is added to gross slope.

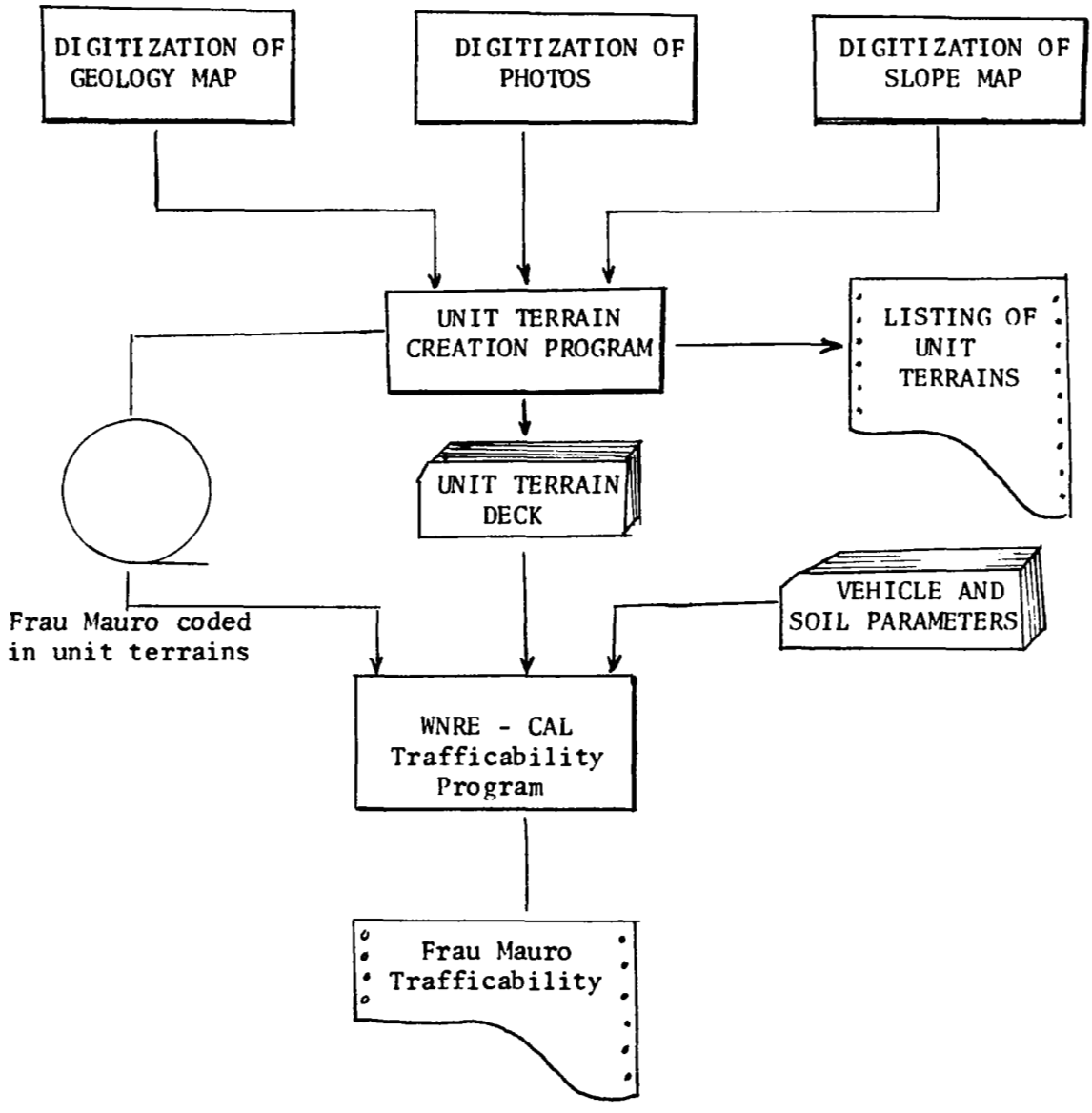

FIGURE I-1

COMPUTER FLOW CHART FOR TRAFFICABILITY ANALYSIS

The rationale behind this procedure is that the inner wall slope for a crater greater than 200 meters in diameter should appear on the slope map. To add the two angles would result in a double counting for large craters. However, as the size of the crater decreases, the likelihood of the inner wall angle being picked up on the slope map decreases. It is therefore necessary to add the angles for craters less than 200 meters in order to more realistically model the degree of difficulty in climbing slopes which would be encountered by objects the size of the vehicle.

It should also be noted that the counts for craters in the 5-20 meter category were not made explicitly in this study. If the input data indicated that a 5-20 meter crater or craters were present, it was assumed that the count was 3. This is a conservative estimate of the mean number which should actually be between 2 and 3. This assumption was made so that compatibility with the WNRE technique of calculating power consumption could be maintained.

The information on the age of craters less than 50 meters in diameter was digitized directly from the geology map. This is a much more efficient technique than that developed for the Sinus Medii analysis.

2. Unit Terrain Output

The following is a listing of the data contained in the unit terrain deck. The percentage figures refer to the percent of the area subjected to the trafficability analysis. From this list we can obtain a coarse characterization of this particular lunar area. For example, Code No. 1-30041110, accounts for 26.2% of the area analyzed. This unit terrain has three old craters in the 5-20 meter category, no blocks, a gross slope of 5°, and a soil firmness index of 1.

CODE NO	UNIT TERRAIN	PERCENT	CUM PERCENT
1	30041110	26.214	26.214
2	30041210	12.589	38.804
3	30041118	9.214	48.018
4	30041310	3.446	51.464
5	30041410	2.857	54.321
6	30041221	2.589	56.911
7	31041110	2.161	59.071
8	30021110	2.018	61.089
9	31041210	1.411	62.500
10	30041222	1.393	63.893
11	30041220	1.357	65.250
12	30041117	1.089	66.339
13	30021440	1.054	67.393
14	31041118	0.982	68.375
15	30021341	0.964	69.339
16	30041116	0.964	70.303
17	30041114	0.911	71.214
18	30041211	0.893	72.107
19	30031110	0.875	72.982
20	999043220	0.786	73.768
21	30031221	0.750	74.518
22	30021210	0.696	75.214
23	30041318	0.679	75.893
24	30021340	0.661	76.553
25	999043110	0.554	77.107
26	30041213	0.554	77.661
27	999043320	0.518	78.178
28	30041223	0.518	78.696
29	30021118	0.518	79.214
30	30021221	0.500	79.714
31	30041218	0.482	80.196
32	30021441	0.446	80.643
33	30041320	0.446	81.089
34	30031222	0.446	81.535
35	31041410	0.429	81.964
36	30041128	0.411	82.375
37	41110	0.411	82.785
38	41210	0.375	83.160
39	31041310	0.375	83.535
40	30031118	0.304	83.839

CODE NO	UNIT TERRAIN	PERCENT	CUM PERCENT
41	30241110	0.304	84.143
42	30041321	0.286	84.428
43	30041212	0.286	84.714
44	31041221	0.268	84.982
45	999043223	0.250	85.232
46	999043222	0.250	85.482
47	999043124	0.250	85.732
48	30041450	0.250	85.982
49	30021144	0.250	86.232
50	30041313	0.250	86.482
51	30031321	0.232	86.714
52	31031221	0.214	86.928
53	31021110	0.214	87.143
54	999033125	0.214	87.357
55	30041315	0.214	87.571
56	30011452	0.214	87.785
57	30041328	0.214	88.000
58	30041115	0.196	88.196
59	30141110	0.196	88.393
60	30021124	0.196	88.589
61	30011110	0.179	88.767
62	1041110	0.179	88.946
63	30041324	0.179	89.125
64	30021222	0.179	89.303
65	30011451	0.161	89.464
66	30041421	0.161	89.625
67	999043210	0.161	89.785
68	999033225	0.161	89.946
69	999043117	0.161	90.107
70	31021341	0.161	90.267
71	31041211	0.143	90.410
72	30031421	0.143	90.553
73	31021210	0.143	90.696
74	30031210	0.143	90.839
75	31041220	0.143	90.982
76	30041323	0.143	91.125
77	41118	0.125	91.250
78	30021126	0.125	91.375
79	30021326	0.125	91.500
80	30021342	0.125	91.625
81	30023440	0.125	91.750
82	30021220	0.125	91.875
83	30021346	0.125	92.000
84	30021321	0.125	92.125
85	30021116	0.125	92.250

CODE NO	UNIT TERRAIN	PERCENT	CUM PERCENT
86	30021421	0.107	92.357
87	31041318	0.107	92.464
88	30021310	0.107	92.571
89	30021246	0.107	92.678
90	30241210	0.107	92.785
91	30241318	0.107	92.892
92	30241218	0.107	92.999
93	31041320	0.107	93.107
94	41213	0.089	93.196
95	21326	0.089	93.285
96	30031310	0.089	93.374
97	31021221	0.089	93.464
98	30041125	0.089	93.553
99	30041225	0.089	93.642
100	30041424	0.089	93.732
101	31041218	0.089	93.821
102	31041117	0.089	93.910
103	21443	0.089	93.999
104	30025440	0.089	94.089
105	30021446	0.089	94.178
106	30141118	0.089	94.267
107	31031210	0.089	94.356
108	30041216	0.089	94.446
109	31041116	0.089	94.535
110	30041215	0.089	94.624
111	31021124	0.089	94.714
112	30031322	0.089	94.803
113	30021322	0.089	94.892
114	41218	0.071	94.964
115	31041222	0.071	95.035
116	32041110	0.071	95.106
117	21126	0.071	95.178
118	999033221	0.071	95.249
119	41225	0.071	95.321
120	30031223	0.071	95.392
121	30031423	0.071	95.464
122	30021442	0.071	95.535
123	31021440	0.071	95.606
124	30241310	0.071	95.678
125	31041212	0.071	95.749
126	30041322	0.071	95.821
127	30021224	0.071	95.892
128	31031322	0.071	95.964
129	30011118	0.054	96.017
130	31031110	0.054	96.071

CODE NO	UNIT TERRAIN	PERCENT	CUM PERCENT
131	41125	0.054	96.124
132	30021410	0.054	96.178
133	31021118	0.054	96.231
134	30041420	0.054	96.285
135	999043310	0.054	96.338
136	21340	0.054	96.392
137	30041418	0.054	96.446
138	30241328	0.054	96.499
139	30023246	0.054	96.553
140	30022440	0.054	96.606
141	141118	0.054	96.660
142	31021144	0.054	96.713
143	21110	0.054	96.767
144	31041215	0.054	96.820
145	31031321	0.054	96.874
146	41124	0.036	96.910
147	32041118	0.036	96.945
148	30021114	0.036	96.981
149	31011118	0.036	97.017
150	30041350	0.036	97.053
151	30141127	0.036	97.088
152	30221110	0.036	97.124
153	30021320	0.036	97.160
154	30011210	0.036	97.195
155	41220	0.036	97.231
156	30011410	0.036	97.267
157	41325	0.036	97.303
158	30041325	0.036	97.338
159	41117	0.036	97.374
160	999043410	0.036	97.410
161	30021128	0.036	97.445
162	1041221	0.036	97.481
163	31041421	0.036	97.517
164	30024440	0.036	97.552
165	30031328	0.036	97.588
166	30024446	0.036	97.624
167	41222	0.036	97.660
168	30041411	0.036	97.695
169	30024246	0.036	97.731
170	30221440	0.036	97.767
171	30021117	0.036	97.802
172	31021340	0.036	97.838
173	33041110	0.036	97.874
174	32041116	0.036	97.910
175	31041223	0.036	97.945
176	30041311	0.036	97.981
177	31031222	0.036	98.017
178	31021218	0.036	98.052
179	31011210	0.036	98.088
180	32041210	0.036	98.124

CODE NO	UNIT TERRAIN	PERCENT	CUM PERCENT
181	31021324	0.036	98.159
182	21210	0.036	98.195
183	30021324	0.036	98.231
184	1041210	0.036	98.267
185	31021441	0.036	98.302
186	41310	0.036	98.338
187	999043118	0.018	98.356
188	31241110	0.018	98.374
189	41313	0.018	98.392
190	30011223	0.018	98.409
191	31031421	0.018	98.427
192	999043211	0.018	98.445
193	999013110	0.018	98.463
194	1141327	0.018	98.481
195	31041450	0.018	98.499
196	999033220	0.018	98.516
197	30021125	0.018	98.534
198	31041225	0.018	98.552
199	32041410	0.018	98.570
200	41320	0.018	98.588
201	999023421	0.018	98.606
202	999043420	0.018	98.624
203	32021110	0.018	98.641
204	31041115	0.018	98.659
205	30031410	0.018	98.677
206	1041117	0.018	98.695
207	30041415	0.018	98.713
208	1021110	0.018	98.731
209	31041315	0.018	98.749
210	30031128	0.018	98.766
211	31011452	0.018	98.784
212	21118	0.018	98.802
213	30021418	0.018	98.820
214	31041328	0.018	98.838
215	30241118	0.018	98.856
216	30021443	0.018	98.874
217	30041422	0.018	98.891
218	31021346	0.018	98.909
219	41211	0.018	98.927
220	31041128	0.018	98.945
221	30025346	0.018	98.963
222	31141110	0.018	98.981
223	21221	0.018	98.999
224	30022446	0.018	99.016
225	30023446	0.018	99.034
226	30022346	0.018	99.052
227	141110	0.018	99.070
228	30241410	0.018	99.088
229	30024346	0.018	99.106
230	30023346	0.018	99.123

CODE NO	UNIT TERRAIN	PERCENT	CUM PERCENT
231	30025246	0.018	99.141
232	30224246	0.018	99.159
233	31022246	0.018	99.177
234	30022246	0.018	99.195
235	30223246	0.018	99.213
236	30031246	0.018	99.231
237	31031117	0.018	99.248
238	31022440	0.018	99.266
239	31023440	0.018	99.284
240	30012451	0.018	99.302
241	30231110	0.018	99.320
242	31041150	0.018	99.338
243	1041118	0.018	99.356
244	30011318	0.018	99.373
245	30241223	0.018	99.391
246	30021223	0.018	99.409
247	30241114	0.018	99.427
248	31041312	0.018	99.445
249	30021231	0.018	99.463
250	31241223	0.018	99.481
251	31021342	0.018	99.498
252	30041312	0.018	99.516
253	31031310	0.018	99.534
254	21342	0.018	99.552
255	2041110	0.018	99.570
256	31041412	0.018	99.588
257	30041412	0.018	99.606
258	1031222	0.018	99.623
259	41116	0.018	99.641
260	32021222	0.018	99.659
261	32041313	0.018	99.677
262	31041321	0.018	99.695
263	1041212	0.018	99.713
264	31221	0.018	99.730
265	31241221	0.018	99.748
266	41221	0.018	99.766
267	1041116	0.018	99.784
268	31021220	0.018	99.802
269	30041150	0.018	99.820
270	30031220	0.018	99.838
271	31041323	0.018	99.855
272	1011210	0.018	99.873
273	31021222	0.018	99.891
274	1041310	0.018	99.909
275	32041321	0.018	99.927
276	32041320	0.018	99.945
277	41323	0.018	99.963
278	32021210	0.018	99.980
279	32021322	0.018	99.998

3. WNRE-CAL Trafficability Computer Model

This is the current version of the trafficability model originally developed by WNRE.* It has been modified to utilize the extra capacity of the CAL IBM 360 model 65 computer over WNRE's IBM 1130. These modifications have dealt mainly with increased use of core storage and high speed printer facilities.

The only significant change in calculation techniques has been the substitution of a modified vehicle-slope analysis for WNRE's straight-and-level computations for unit terrains which contain no craters smaller than 50 meters (see Appendix III). These changes are shown schematically in Figure I-2. In the event that there are no craters smaller than 50 meters in a unit terrain, a table look-up is performed, given slope and soil type, to yield slip, required torque, and power consumption. If slip is less than 70% and required torque less than available vehicle torque, then the power consumption from the table is assigned to the unit terrain code. If the vehicle fails either test, the unit terrain is classified as very difficult to traverse. The logical flow of this program change is illustrated by the following flow diagram.

The tables of Appendix III give us information for soft and firm soil. The computer program considers soil classes 1, 2 and 3 to be firm, while classes 4, 5 and 6 are soft. Obviously, the slope values are derived from the gross slope indicator.

---

* W.C. Grenke and C.J. Nuttall, Jr., Accessibility of Specific Areas on the Lunar Surface as a Function of LRV Design Parameters, Report No. 201, WNRE, Inc, Chestertown, Md., June 1970.

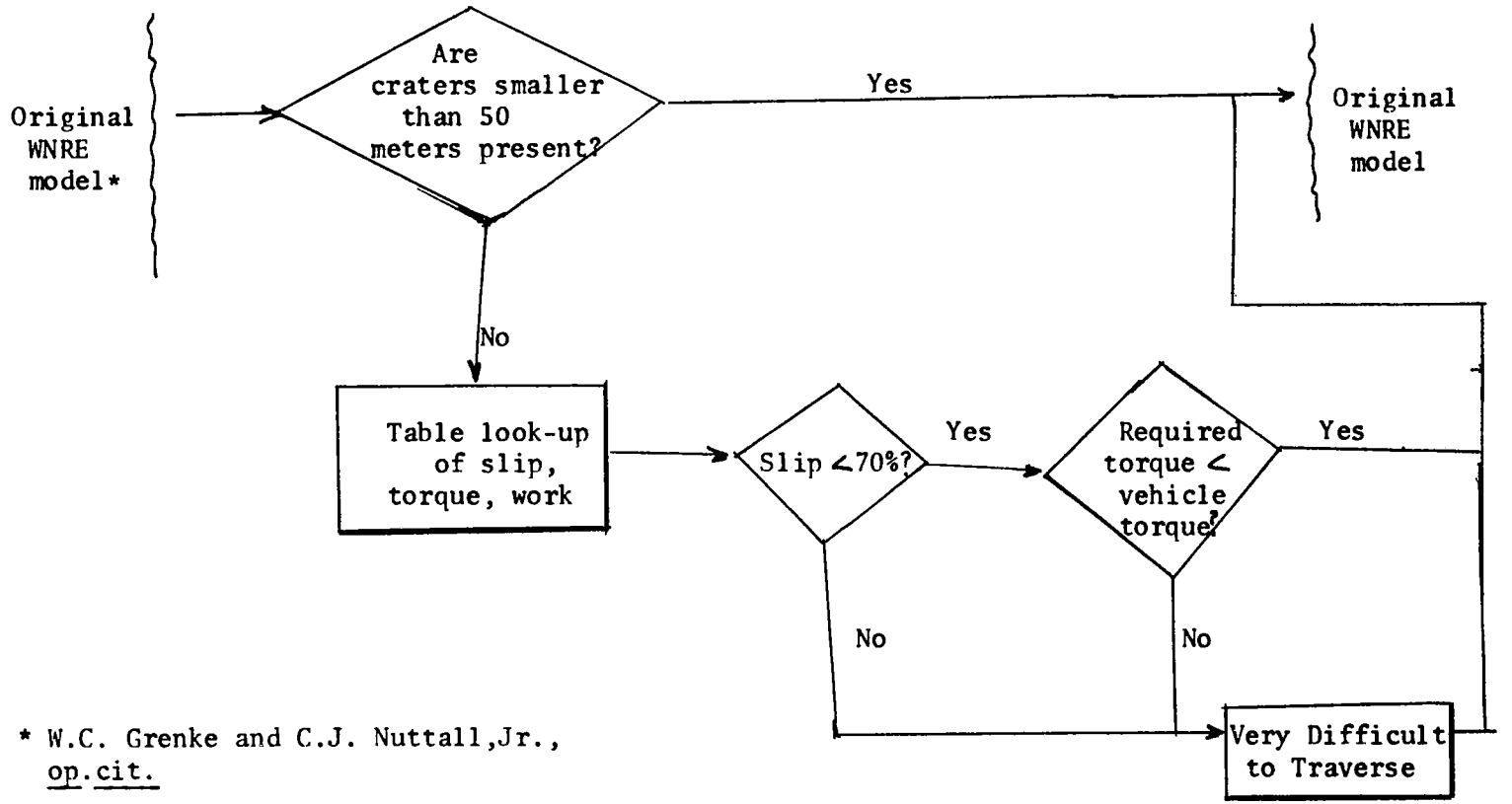

* W.C. Grenke and C.J. Nuttall,Jr., op.cit.

FIGURE I-2

MODIFICATION OF VEHICLE-SLOPE ANALYSIS

APPENDIX II

LANDMARK VISIBILITY COMPUTER PROGRAM DOCUMENTATION

Figure II-1 is a flow chart showing the interrelation of inputs and outputs for the visibility computer model. Data obtained by digitization of a topographic contour map must first be smoothed by means of a "Blending Program" before being fed to subsequent computer operations. Preprocessed landmark inputs must also be incorporated before the basic ASTERISK model for line-of-sight analysis can be employed.

1. Blending Program

The algorithm utilized by the blending program is essentially a technique for performing a linear blending of the input elevations from left to right, then from top to bottom, with the final elevation resulting from averaging the blended values.

Confining our discussion initially to the linear blending in a particular direction, our digitization process presents us with a perplexing problem.

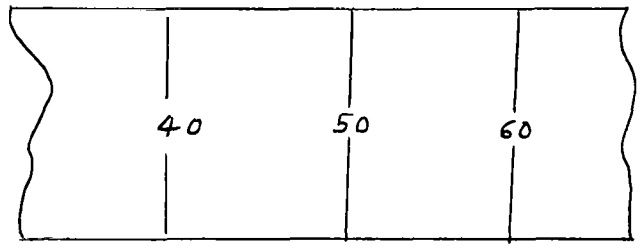

Given the contour map above, we would expect to encounter a digitized profile similar to that shown in Figure II-2(a).

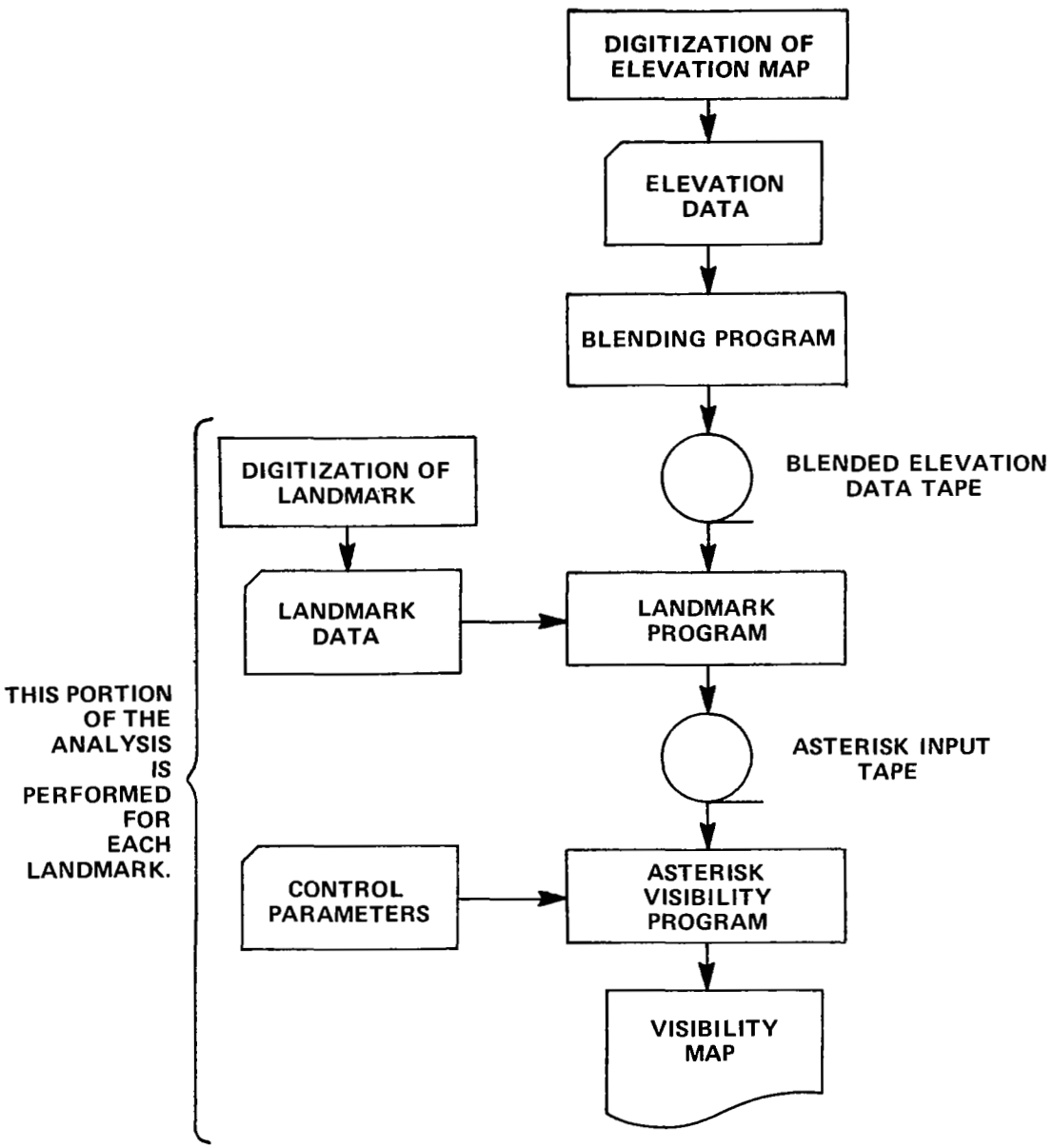

Figure II-1 COMPUTER FLOW CHART FOR VISIBILITY ANALYSIS

FIGURE II-2
DIGITIZING OF PROFILES

Unfortunately, due to our inability to precisely determine elevations between contour lines, the data were recorded as shown in Figure II-3.

FIGURE II-3
VIEWING CONSTRAINTS OF DIGITIZED PROFILE

Figure II-3(a), where X's indicate a point visible from the eye, illustrates the desired result of a visibility analysis of the contour map. Figure II-3(b) shows what happens when the raw digitized data are subjected to visibility analysis. In this figure, the 0's represent points which would be visible with an accurate profile, but which are masked by our digitization process. It is obvious that the invisibility of the 0's is an artifact of our digitization process.

In order to solve this problem, we need to construct a line through the midpoints between the contour lines and adjust the data accordingly. Figure II-4 illustrates the results of this procedure.

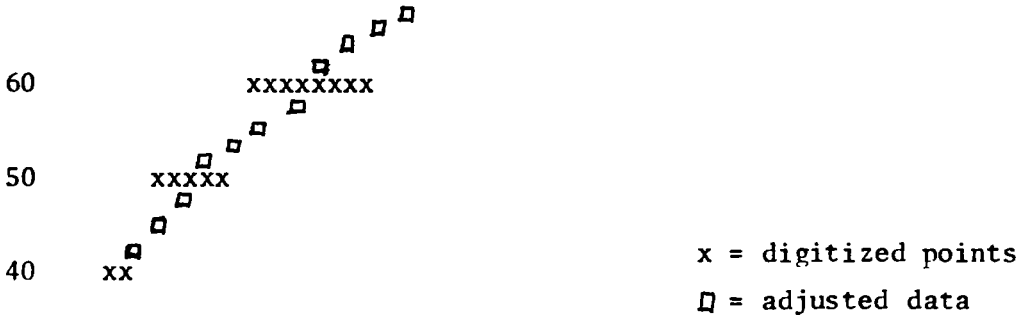

FIGURE II-4
ADJUSTMENT OF PROFILE DATA

We have now replaced our plateaus by linear ramps. Performing this blending in two directions and averaging the results has produced satisfactory blending of the elevation data for the Frau Mauro area of lunar terrain. This is illustrated by the results of visibility analyses performed on a 100 x 100 point test array without blending (Figure II-5) and with blending (Figure II-6).

Note the manner in which the plateaus in the digitized inputs are clearly discernable in the analysis of the unblended data. This problem seems to be alleviated by the blending process as evidenced by the visibility analysis of the blended elevation matrix.

It should be pointed out that the blending procedures from left to right and from top to bottom are performed independently. The resulting elevation is the average of the two independently determined elevation values for any coordinate position. The map data matrix is <u>not</u> first transformed by blending from left to right and then further modified by top to bottom blending to yield the elevation map. The data were blended in the manner indicated to eliminate the possibility of biasing the elevation results by the initial choice of direction of blending.

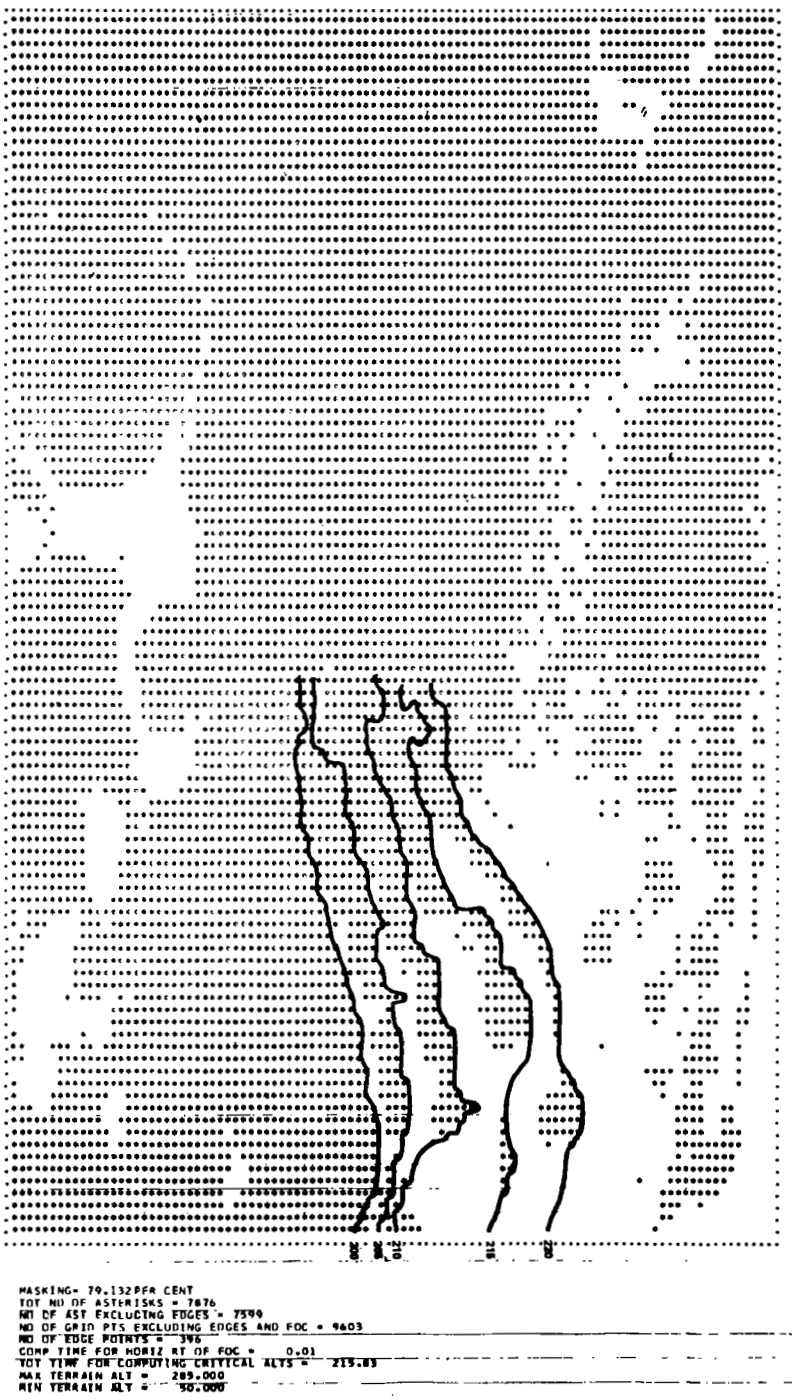

Figure II-5 VISIBILITY ANALYSIS OF UNBLENDED DATA 100 x 100 TEST ARRAY

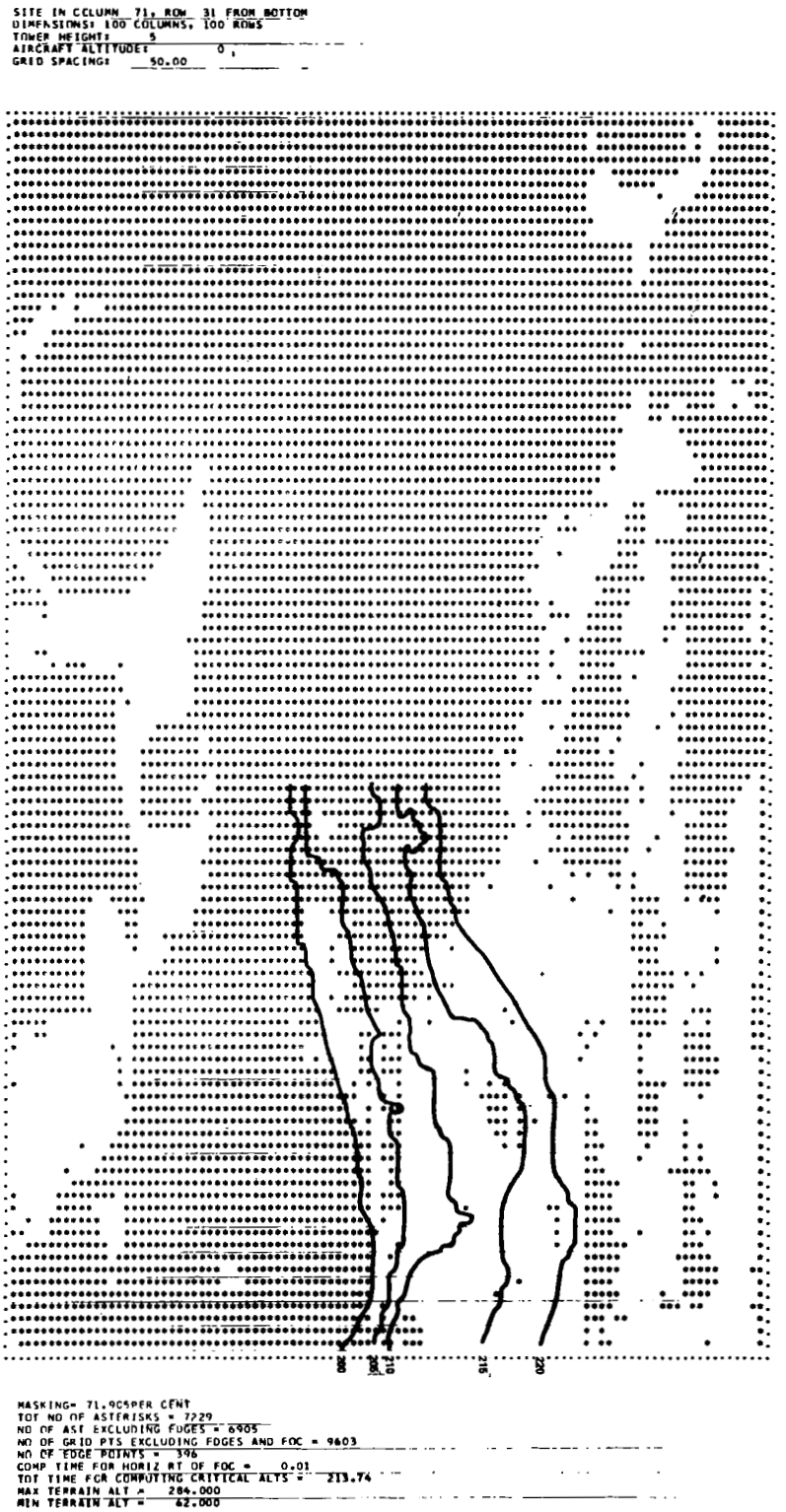

Figure II-6 VISIBILITY ANALYSIS OF BLENDED DATA 100 x 100 TEST ARRAY

2. Landmark Computer Program

This program merely modifies the input data tape for the ASTERISK visibility program to take into account the areal nature of the landmark.

We have adopted a type of truncated flag pole technique for preprocessing the input elevation data so that the ASTERISK model's single sighting point analysis can be expanded to accommodate areal landmark features. If we have a hilltop landmark, we proceed as follows:

(1) By analysis of map data, decide which points are actually on the landmark, and which points fall on the same lunar surface feature as the landmark (see Figure II-7).

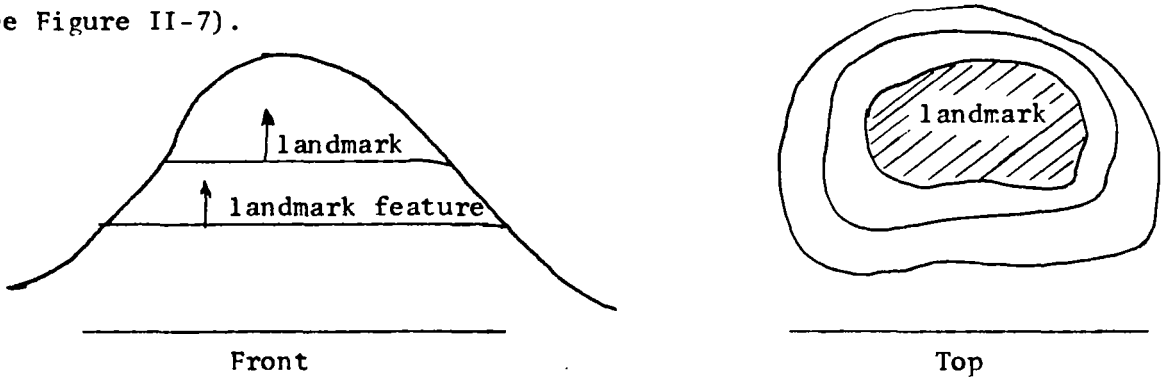

FIGURE II-7
REPRESENTATION OF LANDMARK

(2) Construct a flagpole at the same X, Y position as the landmark peak (see Figure II-8). Set the elevation of the flagpole as the lowest elevation of any landmark point. Set all other points on the landmark equal to 1, and all remaining points on the landmark feature to 2.

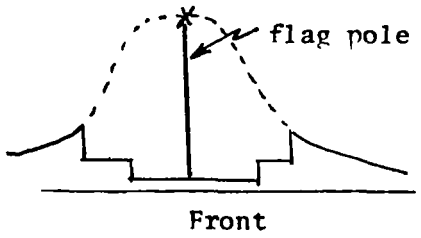

FIGURE II-8
IDEALIZATION OF LANDMARK FOR COMPUTER INPUT

(3) Now the single sighting point ASTERISK program can be run on this preprocessed data to yield a good picture of the landmark visibility.

It should be pointed out that all the points specified as 1's or 2's in (2) above must be determined and decided upon by map interpretation. This is a manual job which the computer cannot determine by itself. It is a task which requires a geographer's expertise.

The ASTERISK program has been modified to incorporate this landmark feature and to output a magnetic tape storage of the visibility situation from any particular feature. The intersection of the data on these output tapes yields an excellent determination of the visibility of various combinations of landmarks from any lunar surface square.

One final point should be noted. The actual landmark derived from our flagpole approach will be a little larger and the visibility requirements therefore a bit more stringent than those actually specified. If we consider the actual and specified feature, this discrepancy is obvious, as shown in Figure II-9 below.

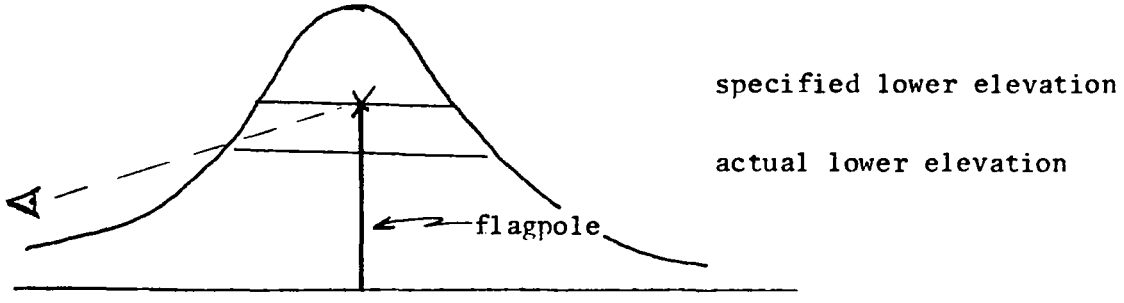

FIGURE II-9

VISIBILITY CONSIDERATIONS FOR IDEALIZED LANDMARK

However, the degree of this error is parametrically controllable by varying the flagpole height, and it should not be significant in any of the analyses performed for this study.

3. ASTERISK Computer Model

The ASTERISK model graphically portrays regions of point-to-point intervisibility in a geographical area. Specifically, for each point of the area the height of the terrain mask as viewed from a fixed observation tower is computed. ASTERISK divides points of the geographic region into two categories: (1) points at which the height of mask exceeds a selected threshold (usually represented by an asterisk; hence the program name); (2) points at which the height of mask does not exceed the threshold (usually represented by a blank).

With respect to a chosen observation point (tower) the height of mask from any other point P on the terrain is the altitude to which an object at P must be raised to be just visible to the observer in the tower. This concept is shown in Figure II-10. Here point P is not visible to the observer and the degree of masking is indicated by the height (maybe depth would have been a better word) of mask. Point Q is visible to the observer. Its height of mask is zero.

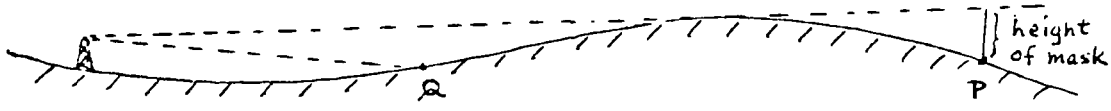

FIGURE II-10
HEIGHT OF MASK

As input, the model uses terrain heights at the points of intersection of a square grid placed on a map of a rectangular geographical area. The choice of grid size and size of the rectangular region is usually a compromise involving a number of factors:

(1) The desired region of interest.

(2) The roughness of the terrain (rougher terrain requires a finer grid to avoid loss of important details, especially of ridges and peaks).

(3) The amount of core storage available (packing of two or three heights in a single word should be considered).

(4) Computer charges for running the program.

Figure II-11 shows a sample grid with terrain heights at each point of intersection. It also shows the location of an observation tower at 0 and a point P whose height of mask is to be computed.

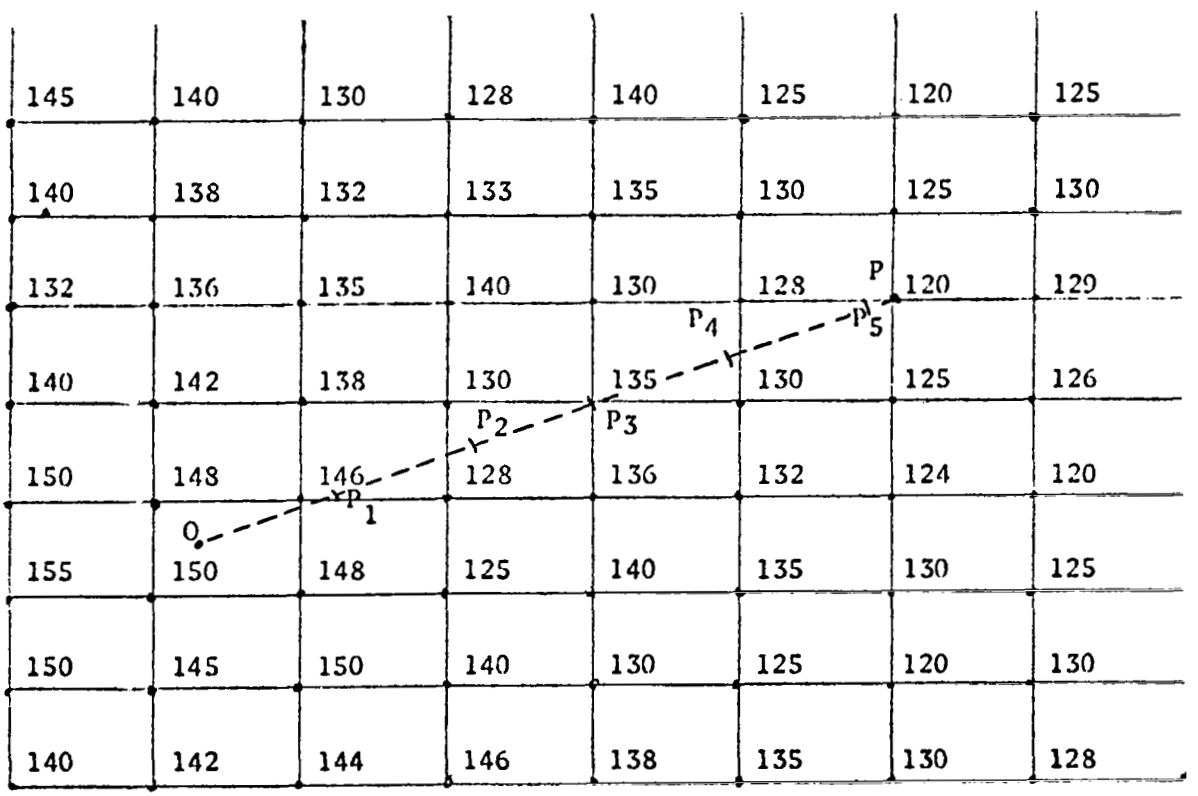

FIGURE II-11

TERRAIN GRID

First, we obtain the profile of the terrain over the path joining 0 to P. This is done by placing a set of intermediate points (P_1, P_2, ...) between 0 and P marked off in equal spacings from 0 toward P. The last interval will not necessarily be equal to the others. The height of the terrain at each of these points (0, P_1, P_2, ...) is then estimated by an interpolation process on the input terrain data. Specifically, the model uses a bilinear interpolation on the heights at the four corners of the square in which the point falls, and takes into account the position of the point within the square. More elaborate interpolative schemes could be used. The one drawback of the bilinear method is that the height of the intermediate point never exceeds the maximum of the four corner heights.

After the interpolated profile has been obtained it will represent a series of spikes, as shown in Figure II-12. This has been obtained from flat terrain map data and needs to be corrected for terrain curvature if the distances involved are long. Specifically, the model corrects only if the distance exceeds 1 milliradian of arc on the moon's assumed spherical surface.

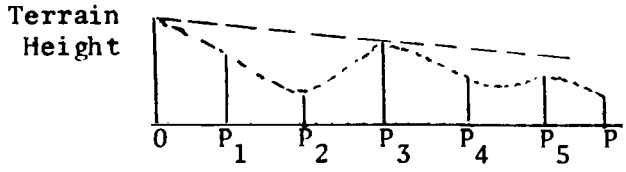

FIGURE II-12

INTERPOLATED PROFILE

Figure II-13 shows an exaggerated drawing of how the interpolated profile might look after correction for curvature.

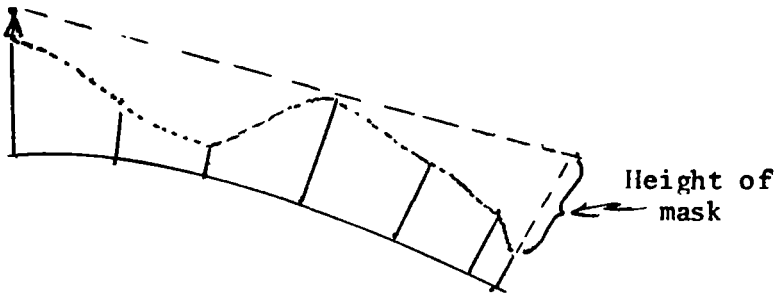

FIGURE II-13

CURVATURE CORRECTED PROFILE

At this point in the process, lines are drawn from the top of the observation tower to the top of each of these spikes and the line having maximum angle of elevation (or smallest angle of depression) is saved for the height of mask computation. In Figure II-13 the line to top of P_3 has the smallest angle of depression. The distance from the top of P to this line measured radially outward is called the height of mask for point P with respect to the observation point O. It is obviously a function of the height of the observer above the terrain.

The process described for point P is repeated for all other grid points, keeping the observation point O in the fixed location. At the end of the computation one has the height of mask for each point of the grid. Rather than print out this array of numbers, the model groups the values into class intervals, with the letter A representing values in the first class interval, B representing heights of mask in the second class interval, and so on, continuing on through Y for those heights of mask in the twenty-fifth class interval. The letter Z is reserved for heights of mask greater than 25 class intervals in magnitude. The output is a rectangular array of letters, sometimes quite thoroughly mixed.

The array of mask heights obtained from the above calculation need not be printed out if only a presentation of masked versus unmasked area is desired. Rather, the information is stored on tape for subsequent use. The model tests

each height of mask against a desired threshold and prints an asterisk for points having masks deeper than the threshold and leaves a blank for points having masks shallower than the threshold. A number of different thresholds can be examined and an asterisk print-out obtained for each threshold.

APPENDIX III

VEHICLE SOFT-SOIL PERFORMANCE MODELING

by

D. J. Schuring

The mathematical model is derived under the following simplifying assumptions:

1. The vehicle is moving on a straight course with constant speed so that turning maneuvers and side forces are excluded.
2. The ground is relatively smooth so that pitching, heaving, rolling, etc. can be neglected.
3. The ground is soft but relatively firm so that phenomena resulting from excessively weak soils are not considered.
4. As a consequence of (1) and (2), vehicle forces are restricted to a plane. This plane is identical with the wheel plane. Moments are applied in a direction perpendicular to this plane (bicycle-type vehicle).

Since inertia forces are neglected, the only force acting at the vehicle's cg is its weight, which is counter-balanced by forces acting in the vehicle-ground interface. Figure III-1 shows a two-dimensional free-body diagram of a wheeled vehicle moving up-hill with constant speed over soft, smooth ground. The vehicle maintains force equilibrium against motion-impeding forces by generating thrust forces, $\sum_{1}^{4} H_i$, at the driven wheels. The impeding force is the weight component, $\overline{W} \sin \alpha$. H_1 and H_2 are the thrust forces of the front wheels; H_3 and H_4 are the thrust forces of the rear wheels. $\overline{W}$ is the total vehicle weight.

Consequently,

$$\sum_{1}^{4} H_i = \bar{W} \sin \alpha \tag{1}$$

Equation (1) can be considered the "demand" equation of a wheeled vehicle. Its terms are furnished by examining forces and moments of a single wheel, Figure III-2. If the wheel is driven (M>0), the horizontal force at the soil-wheel interface is directed forward and identical with the thrust, H. Equilibrium requires that for each wheel

$$\frac{M}{r} = V\rho + H \tag{2}$$

where $\rho = f/r$ is called the coefficient of rolling resistance, and V is the wheel load normal to the ground. Eq. (2) substituted into Eq. (1) yields

$$\sum_{1}^{4} \frac{M_i}{r_i} = \sum_{1}^{4} V_i \rho_i + \bar{W} \sin \alpha \tag{3}$$

Assuming constant coefficient of rolling resistance and constant wheel radius for all four wheels, this equation simplifies to

$$\bar{M} = \bar{W} r \cos \alpha \left(\rho + \tan \alpha\right) \tag{4}$$

where $\bar{W}$ is the total vehicle weight, and $\bar{M}$ the total driving torque.

The torque is furnished by the drive motors. In order to match torque demand and torque supply (which is dependent on the wheel speed), the wheel slip has to be estimated.

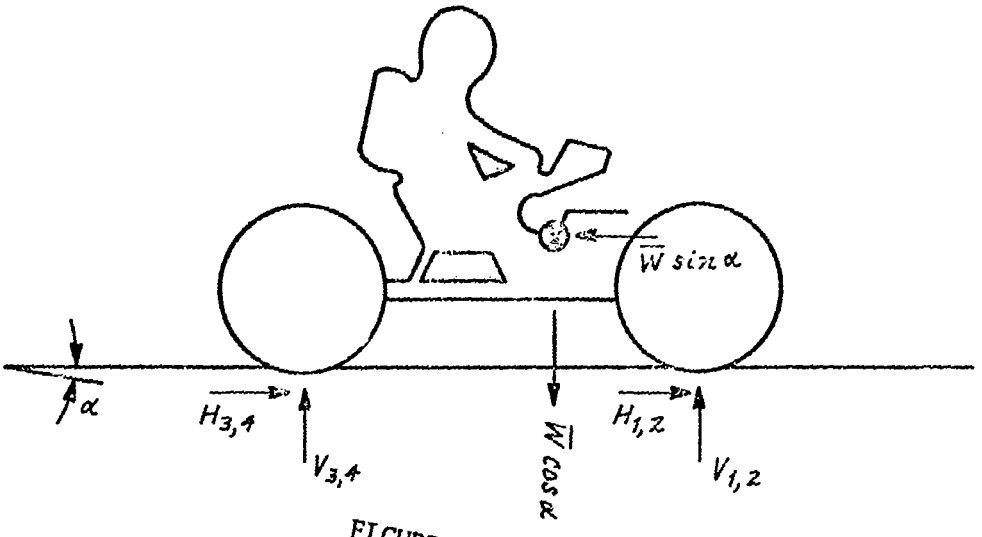

FIGURE III-1

FREE-BODY DIAGRAM OF VEHICLE

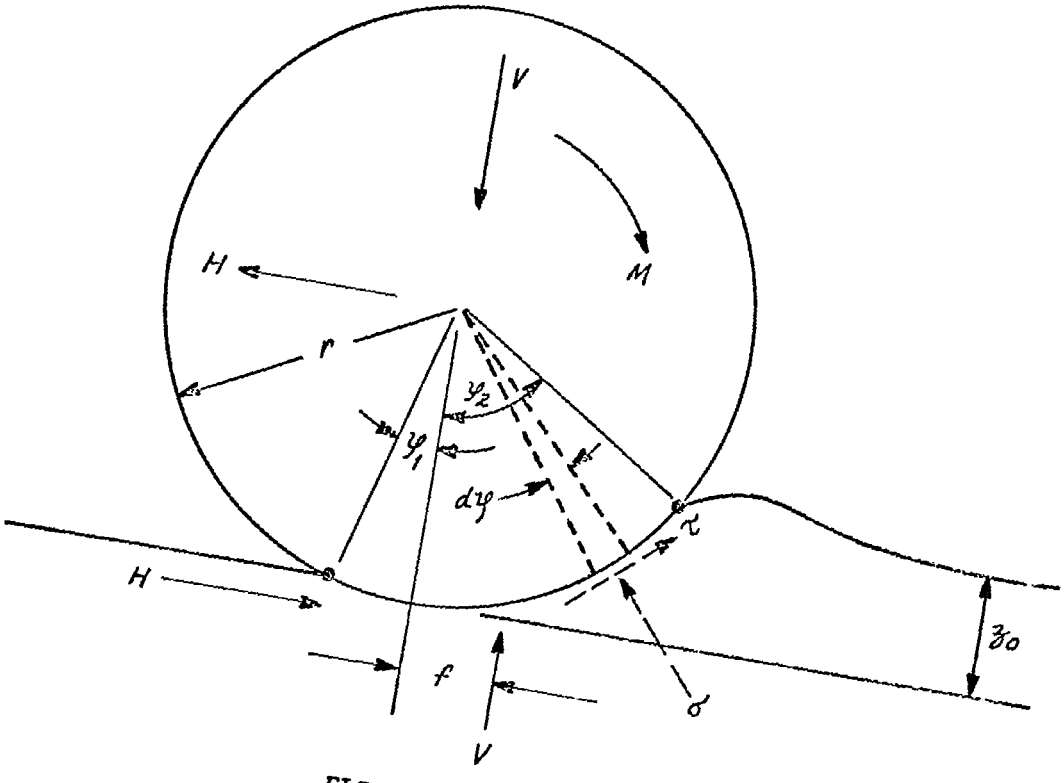

FIGURE III-2

FREE-BODY DIAGRAM OF i-th WHEEL
(INDICES "i" ARE OMITTED)

Computation of slip:

The torque, M, of a wheel is equal to the sum of all tangential forces along the contact zone times their distance, r, from the wheel axle (Figure III-2).

$$M = r \int_{(A)} \tau \, dA \tag{5}$$

where τ is the interface shear stress, and A is interface area.

If the interface shear stress, τ, is uniformly directed in forward direction (this is generally true), the Janosi-Hanamoto equation [1]* can be applied.

$$\tau = (c + \sigma \tan \phi)\left(1 - e^{-\frac{d}{k}}\right) \tag{6}$$

where c is soil cohesion, ϕ is internal soil friction angle, σ is normal interface stress, d is displacement of wheel versus soil in the interface, and k is a soil constant. For relatively small sinkage, σ can be approximated by

$$\sigma \approx \frac{W \cos \alpha}{A} \tag{7}$$

where W is the vehicle weight per wheel.

Furthermore, the displacement can be approximated by [2]

$$d \approx r s (\gamma_2 - \gamma) \tag{8}$$

where γ_2 is the front angle (Fig. III-2) and s is wheel slip given by

$$s = 1 - \frac{v}{r\omega} \tag{9}$$

---

* numbers refer to references at the end of this Appendix.

v is forward velocity of the wheel, and ω is angular wheel velocity.

With Eqs. (7) and (8), the shear-stress equation, Eq. (6), takes the form

$$\tau = \left(c + \frac{W \cos\alpha}{A} \tan\phi\right)\left(1 - e^{-\frac{rs}{k}(\theta_2 - \theta)}\right) \tag{10}$$

If we assume rectangular contact area with width b, then $dA = b\,r\,d\theta$.

If we further assume the rear contact angle, θ_1 to be zero (Figure III-2), then, with Eq. (10) substituted into Eq. (5), the torque, M, of a wheel becomes

$$M = r^2 b \left(c + \frac{W}{A} \cos\alpha \tan\phi\right)\int_0^{\theta_2}\left(1 - e^{-\frac{rs}{k}(\theta_2 - \theta)}\right) d\theta \tag{11}$$

Integration yields

$$M = r^2 b\,\theta_2 \left(c + \frac{W}{A} \cos\alpha \tan\phi\right)\left[1 - \frac{k}{r\theta_2 s}\left(1 - e^{-\frac{r\theta_2 s}{k}}\right)\right] \tag{12}$$

Let us call $r\theta_2 \equiv L$ the contact length, and let us also define the contact width as $b = A/L$. Then

$$M = Wr \cos\alpha \left(\frac{c}{p} + \tan\phi\right)\left[1 - \frac{k}{Ls}\left(1 - e^{-\frac{Ls}{k}}\right)\right] \tag{13}$$

where $p = \dfrac{W \cos\alpha}{A}$ is the average wheel pressure.

Eq. (13) cannot be solved without estimation of the contact length, L. Here, we will assume that the contact length of a wheel rolling slowly on soft soil equals the contact length of the same wheel standing on rigid ground. This is a drastic assumption; it is justified only if the ground is rather firm so that wheel sinkage is small and wheel deformation large.

Figure III-3 shows the deformation of an elastic wheel standing on rigid ground and loaded by $W \cos \alpha$, where W is the vehicle weight per wheel, and α is the slope angle. Wheel deflection and contact length are related according to the expression

$$L = \sqrt{8 r_o \Delta} \tag{14}$$

W.C. Grenke and C.I. Nuttall [3] quote the following empirical load-deflection relation for a single lunar-vehicle wheel

$$\underset{\text{(meter)}}{\Delta} = 8.8 \times \underset{\text{(Newton)}}{V}^{0.75} 10^{-4} \tag{15}$$

where V is the wheel load normal to the ground. With $V = W \cos\alpha$, and $r_o = 0.406$ meters, Eq. (15) substituted into Eq. (14) yields

$$L_{(meter)} = \frac{\left[W_{(Newton)} \cos \alpha\right]^{0.375}}{18.7} \tag{16}$$

W.C. Grenke and C.I. Nuttall [3] also quote an empirical relation between normal wheel load, V, and average contact pressure,

$$p = 800 \sqrt[3]{V} \tag{17}$$

Since $V = W \cos \alpha$, this relation can be expressed as

$$p = 800 \sqrt[3]{W \cos \alpha} \tag{18}$$

where W is the vehicle weight per wheel.

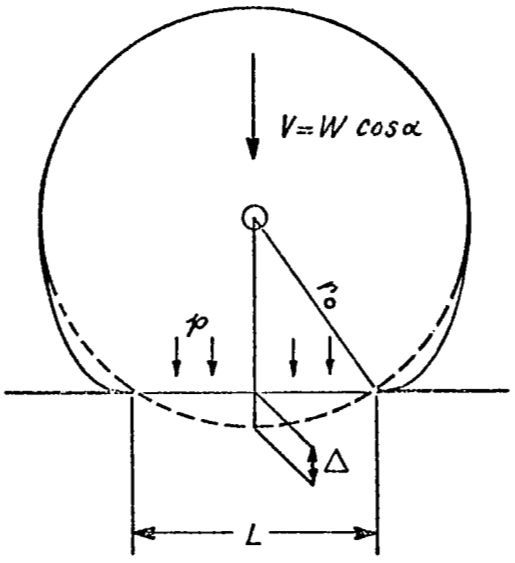

FIGURE III-3

WHEEL CONTACT LENGTH ON RIGID GROUND

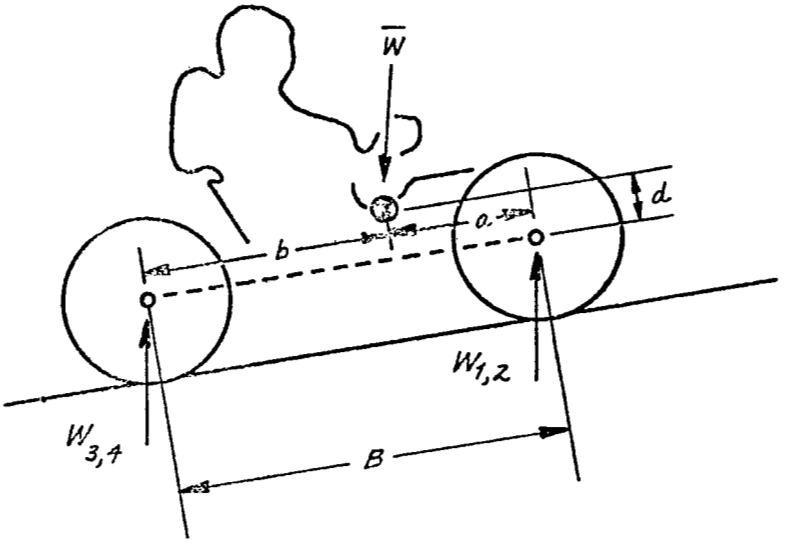

FIGURE III-4

VEHICLE DIMENSIONS

Eqs. (16) and (18) substituted into Eq. (13) yield the necessary torque per single wheel as a function of wheel slip,

$$M = Wr\cos\alpha\left[\frac{c}{800\sqrt[3]{W\cos\alpha}} + \tan\phi\right]\left[1 - \frac{18.7K}{S(W\cos\alpha)^{0.375}}\left(1 - e^{-\frac{S(W\cos\alpha)^{0.375}}{18.7K}}\right)\right] \quad (19)$$

For terrestrial soils, the soil constant $K \approx 0.025\ m$. The same value may be assumed for lunar soils.

We now turn back to Eq. (4) and refer it to a single wheel

$$M = Wr\cos\alpha\,(\rho + \tan\alpha) \quad (20)$$

Comparing Eq (20) with Eq (19) we arrive at

$$\rho + \tan\alpha = \left[\frac{c}{800\sqrt[3]{W\cos\alpha}} + \tan\phi\right]\left[1 - \frac{0.47}{S(W\cos\alpha)^{0.375}}\left(1 - e^{-\frac{S(W\cos\alpha)^{0.375}}{0.47}}\right)\right] \quad (21)$$

The vehicle weight per wheel, W_1, is a function of slope. Figure 4 shows that

for a front wheel $$W_1 = W_2 = \overline{W}\,\frac{b\cos\alpha - d\sin\alpha}{2B\cos\alpha} \quad (22)$$

for a rear wheel $$W_3 = W_4 = \frac{\overline{W}}{L} - W_1 \quad (23)$$

Vehicle data: (see Table III-1)

Wheel base B = 2.28 meters

cg distance from front axle a = 1.26 meters

cg distance from rear axle b = B-a = 1.02 meters

cg vertical height above axle d = 0.41 meters

total lunar vehicle weight $\overline{W}$ = 1015 Newtons (full load)

TABLE III-1 - VEHICLE DATA AS SPECIFIED BY NASA

ITEM		Dimension	Denotation	
			Nuttall[3]	This report
Lunar gross vehicle weight (full payload)	1015	Newton	VW	$\overline{W}$
Lunar net vehicle weight	343	Newton		
Lunar weight of single wheel	17.8	Newton		
Wheel base (axle to axle)	2.28	meter	VL	B
Wheel tread (center to center)	1.83	meter	VTW	
Distance of vehicle cg from front axle*	1.26	meter	VCL	a
Height of cg from level ground (nominal)	.832	meter	VCH	
Height of cg above axles	.41	meter		d
Ground clearance (full load)	.356	meter	VGC	
Wheel diameter	.813	meter	VWD	2r
Wheel width	.228	meter	VWW	
Angle of approach	35	degree	VAA	
Angle of departure	90	degree	VAD	
Maximum step height (μ=0.6)**	.30	meter	VSH	
Maximum crevice width (μ = 0.6)	.70	meter	VMC	
Gradeability	25	degree	VG	
Max. Wheel torque(continuous duty at 35 rpm)	106	N-m	VT	$\overline{M}_{max}$
Max. wheel speed (at 6.8 N-m)	118	rpm		
Wheel spring rate (front and rear)	56 .	N/cm		
Suspension spring rate (front and rear)	25.5	N/cm		
Max. suspension deflection	.229	meter		
Minimum turning radius (wall to wall)	3.10	meter		

*computed from given weight distribution of 45% front and 55% rear

** μ = coefficient of friction

Soil data:

The coefficient of rolling resistance, ρ is a complex function of wheel data, soil data, load, and slip. Wheel tests performed on the Boeing-GM Lunar wheel in Yuma sand [4] indicate a coefficient of roll. res. of 0.10 at higher slip and 0.18 at low slip. (WNRE[3] selected a conservative value of ρ = 0.18).

Apollo II soil samples [5] indicate a soil cohersion of C = 0.36 - 1.42 kN/m^2 (0.05 - 0.20 lb/in^2) and an angle of internal soil friction of $\emptyset$ = 35° - 45°. From these data, two extreme soft-soil conditions can be assembled.

TABLE III-2. LUNAR SOIL DATA*

	Cohesion C-kN/m2	Angle of Internal Friction Ø-degree	Coefficient of rolling resistance ρ
Weak soil	≈ 0.36	≈ 35°	≈ 0.20
Firmer soil	≈ 1.42	≈ 45°	≈ 0.10

*adapted from [4] and [5]

These data substituted into Eq. (21) result into two slope-slip equations

weak soil $$\tan\alpha + 0.20 = \left[\frac{1}{2200\sqrt[3]{W_{F,R}\cos\alpha}} + 0.70\right] S \qquad (24)$$

firmer soil $$\tan\alpha + 0.10 = \left[\frac{1}{560\sqrt[3]{W_{F,R}\cos\alpha}} + 1.0\right] S \qquad (25)$$

where

$$S = 1 - \frac{0.47}{S(W_{FR}\cos\alpha)^{0.375}}\left(1 - e^{-\frac{S(W\cos\alpha)^{0.375}}{0.47}}\right) \qquad (26)$$

$$W_F\cos\alpha = 223\,(1.02\cos\alpha - 0.41\sin\alpha) \text{ for front wheels} \qquad (27)$$

$$W_R\cos\alpha = (508 - W_F)\cos\alpha \text{ for rear wheels} \qquad (28)$$

These formulas can be used to compute four lists of associated slip-slope values - two lists (front and rear) for the weak soil, and two lists (front and rear) for the firmer soil. Soil angles range from 0 to 30 degree in 2 degree increments. With these four lists, identification of go-no go performance is achieved as follows **(Table III-3)**.

First, for a given slope, the associated slip value is identified in the slip-slope list. If the slip value is smaller than thirty per cent, the vehicle considered in a "go" situation. If the slip value is larger than 30% but smaller than 80%, the vehicle is considered in a "perhaps go" condition. For slip values larger than 80%, the vehicle is considered stalled. (no go). The slip values of 30% and 80% are conservative limits; they take into account the "hump" that some cohesive soils exhibit in their thrust-slip curve of around 30% slip. Beyond this hump, the thrust conditions are difficult to assess becuase of the wheel's tendency to spin and bog down.

If the slip is smaller than 30%, the torque demand is computed. According to Eq. (4), the total torque is

$$\bar{M} = \bar{W}\, r\, \cos\alpha\, (\rho + \tan\alpha) \tag{29}$$

The maximum vehicle weight is $\bar{W}$ = 1015 Newtons, the estimated radius of the deflected wheel is r = 0.34 meters. The coefficient of rolling resistance for weak soil was assumed ρ = 0.18 and for firmer soil ρ = 0.10. With these data, the total torque demand is:

$$\bar{M} = 346\, \cos\alpha\, (0.18 + \tan\alpha) \qquad \text{for weak soil} \tag{30}$$
$$\bar{M} = 346\, \cos\alpha\, (0.10 + \tan\alpha) \qquad \text{for firmer soil}$$

where α is the slope angle. Eq. (30) results into a list of total torque demand versus slope.

The maximum torque delivered by the power source is $\bar{M}_{max}$ = 106 Newton meters. If the torque demand surpasses this number, the vehicle is considered in a no-go situation. If the demanded torque is smaller than $\bar{M}_{max}$ = 106 Nm, the work per unit distance is computed.

The power required per axle is

$$P = M\omega \tag{31}$$

where M is the torque per axle, and ω is the rotational velocity.

Introducing wheel slip

$$S = \frac{r\omega - v}{r\omega} \tag{32}$$

where r is wheel radius, and v is vehicle speed, the power equation can be expressed as

$$P = \frac{M}{r} \quad \frac{v}{1-S} \tag{33}$$

The total power of both axles is, then

$$\bar{P} = P_{FRONT} + P_{REAR} = \frac{v}{r}\left[\frac{M_F}{1-S_F} + \frac{M_R}{1-S_R}\right] \tag{34}$$

Work is defined as

$$\bar{E} = \bar{P}t \tag{35}$$

where t is elapsed time. For constant vehicle speed, t can be replaced by

$$t = \frac{D}{v} \tag{36}$$

where D is traveled distance. Eqs. (34) and (36) substituted into Eq. (35) yield the work per unit distance

$$\frac{E}{D} = \frac{1}{r}\left[\frac{M_F}{1-S_F} + \frac{M_R}{1-S_F}\right] \tag{37}$$

Results

Slip, drive.torque, and work per unit distance are computed for the Lunar rover traveling over soft smooth ground. Listed in a table, the computed data can be used to rapidly identify "go" and "no-go" conditions as a function of slope. Tables III-4 and III-5 are computed for two types of Lunar soil respectively.

TABLE III-3 - SAMPLE OF LUNAR VEHICLE MOBILITY DATA PRESENTATION

Slope	Front axle			Rear Axle			Total	
	Slip S_F %	torque M_F N-m	Work E_F/D N-m/km	Slip S_R %	Torque M_R N-m	Work E_R/D N-m/km	Torque $\bar{M}$ N-m	Work E/D N-m/km
0	go			go			go	
2 degree increments	30			30			106	
	perhaps go			perhaps go			no go	
	80			80				
30	no go			no go				

SLOPE	FRONT AXLE			REAR AXLE			TOTAL	
degree	Slip S %	Torque M N-m	Work E/D W-s/m	Slip S %	Torque M N-m	Work E/D W-s/m	Torque M N-m	Work E/D W-s/m
0	2	8	23	1	9	28	17	51
2	2	10	31	2	13	39	23	70
4	3	13	38	2	16	50	29	88
6	3	15	46	3	20	61	35	107
8	4	17	53	3	24	73	41	126
10	5	19	60	4	28	85	47	145
12	5	21	67	5	32	98	53	165
14	6	23	74	5	36	111	59	185
16	7	25	81	6	40	124	65	205
18	8	27	87	7	44	139	71	226
20	10	29	93	8	48	154	77	247
22	11	30	100	9	53	170	83	270
24	13	32	107	10	57	187	89	294
26	15	33	113	12	62	206	95	319
28	18	34	121	14	66	227	100	348
30	21	35	130	16	71	250	106	380

Table III-4 - Firm Soil

Slip, torque, and work per unit distance, all as functions of slope angle

E = Work (N-m = W-s)
D = Distance (m)
W = Watt

N = Newton
m = meter
s = second

SLOPE	FRONT AXLE			REAR AXLE			TOTAL	
degree	Slip S %	Torque M N-m	Work E/D W-s/m	Slip S %	Torque M N-m	Work E/D W-s/m	Torque $\bar{M}$ N-m	Work $\bar{E}/D$ W-s/m
0	5	15	48	4	19	58	34	106
2	6	18	56	5	23	70	41	126
4	7	20	64	6	26	82	46	146
6	8	22	72	7	30	95	52	167
8	10	24	80	9	34	109	58	189
10	12	26	88	10	38	124	64	212
12	14	28	97	12	42	140	70	237
14	18	30	107	15	46	158	76	265
16	20	32	118	18	50	178	82	297
18	26	34	133	22	54	204	88	337
20	34	35	157	28	59	240	94	397
22	49	36	210	40	63	309	99	519
24	88	37	881	70	68	663	105	1544
26	100	-	-	100	-	-	-	-
28	100	-	-	100	-	-	-	-
30	100	-	-	100	-	-	-	-

Table III-5 - Weak Soil

Slip, torque, and work per unit distance, all as functions of slope angle

E = Work (N-m = W-s)
D = Distance (m)
W = Watt

N = Newton
m = meter
s = second

REFERENCES (APPENDIX III)

[1] Janosi, Z.J., B. Hanamoto: The analytical determination of drawbar pull as a function of slip for tracked vehicles in deformable soils. In: Proc. 1st Internat. Conf. Mech. Soil-Vehicle Systems, Turin, 12. bis 16. Aug. 1961. Turin: Edizioni Minerva Technica 1962 pp. 707/36.

[2] Schuring, D.: The energy loss of a wheel. In: Proc. 2nd Internat. Conf. Internat. Soc. Terrain-Vehicle Systems, 29 Aug. bis 2 Sept. 1966. Quebec City, Canada: Univ. Toronto Press 1966; pp. 391/424.

[3] Grenke, W.C., C.J. Nuttak, Jr.: Accessibility of specific areas on the lunar surface as a function of LRV mobility design parameters. WNRE, Chestertown, Maryland. Conducted for NASA MSFC, Huntsville, Ala (June 1970).

[4] Freitag, D.R., et al.: Performance evaluation of wheels for lunar vehicles.U.S. Army Corps of Engineers WES, Vicksburg, Miss. Conducted for NASA MSFC Huntsville Ala. Rep. No. M-70-2 (March 1970).

[5] Costes, N.C. et al.: Apollo II soil mechanics investigations, Science 167 (3918) pp. 739-741 (Jan 1970).